International Journal of Bifurcation and Chaos

https://doi.org/10.1142/S0218127426300302

Synthesis of Dynamical Systems with Chaotic Attractors

Anton V. Doroshin & Nikolay A. Elisov

Research Laboratory of Aircraft Flight Dynamics and Control, Samara National Research University, Moskovskoe sh. 34Samara, 443086, Russia[*]

doran@inbox.ru; mr07th@gmail.com.com

https://www.worldscientific.com/doi/epdf/10.1142/S0218127426300302

This paper discusses dynamical system synthesis with strange chaotic attractors. Such dynamical systems have abstract mathematical meaning but can be used to solve different applied problems. Two approaches for the formation of strange attractors are proposed. The first approach is a direct approach based on searching the coefficients of the nonlinear differential equation system that satisfy the required conditions for Lyapunov exponents and Kaplan-Yorke dimension. The second approach is an indirect approach based on methods and models of spacecraft attitude dynamics. The search for strange attractors is conducted using the differential evolution algorithm. Some new strange attractors are synthesized and analyzed. The analysis involves obtaining Lyapunov exponents, Kaplan-Yorke dimensions, and bifurcation diagrams.

Keywords: dynamical chaos; chaotic strange attractor; bifurcation; differential evolution; spacecraft; attitude dynamics

1. Introduction

The multifaceted study of chaotic phenomena has been and remains one of the broadest current topics. The first prerequisites for the foundation of chaos theory were laid by James Clerk Maxwell [1995]. He discussed complex phenomena in which instabilities may occur, using the example of double refraction of light. When solving the three-body problem, Henri Poincaré noticed and discovered that a slight change in the initial conditions leads to their trajectories moving rapidly away from each other [Poincaré, 2017]. As it is known, the phenomenon of dynamical chaos was first discovered by Lorenz in 1963 when he studied atmospheric convection [1963]. The same model was obtained by Haken in 1975 to explain the phemomenon of irregularly spiking lasers [Haken, 1975]. In 1976, Rössler [1976] derived a dynamical system with a strange attractor, which has only one nonlinear term. In 1984, Matsumoto discovered a chaotic attractor in a simple autonomous circuit [1985; 1986; 1987]. Later, the existence of a chaotic attractor in an electrical circuit was proved experimentally [Zhong & Ayrom, 1985]. In addition, the existence of the hidden attractor based on Chua's circuit was confirmed [Kuznetsov *et al.*, 2023]. In 2012, Sprott proposed a system of ordinary differential equations (ODE) with strange attractors [Elhadj & Sprott, 2013].

[*]Author for correspondence.

Owing to the significant interest in strange chaotic attractors in dynamical systems and the complex dynamical behavior they exhibit, an interesting problem has arisen regarding the deliberate creation of such attractors in various types of systems, including their automatic generation.

Sprott was one of the first to propose the automatic generation of a strange attractor algorithm [1993]. He considered the quadratic map and suggested randomly sorting the mapping coefficients and initial conditions until the Lyapunov condition is fulfilled. Later, a similar approach was expanded for ODE [Sprott, 1994; Sprott, 1997; Li & Sprott, 2013], trigonometric functions [Li & Sprott, 2017], and hyperchaotic systems [Sprott, 2000]. Based on Sprott's attractors, Wang and Chen [2013] proposed the methodology of strange attractors generation with equilibrium points. Similar problems were discussed in [Yang & Qiao, 2019]. The paper [Yang & Qiao, 2019] presents a methodology for constructing simple analytical chaotic systems. Also, this problem was solved for strange attractors with an infinite number of equilibrium points [Pham et al., 2016; Mobayen et al., 2018].

Another way to generate a strange attractor is Chua's circuit. To provide the chaotic behavior, Chua's circuit must contain at least one nonlinear element, one locally active resistor, and three energy-storage elements [Kennedy, 1993]. One of the first modifications of Chua's circuit was proposed in 1994 by Zhong [Zhong, 1994]. He replaced Chua's diode by the cubic polynomial to eliminate the losses due to piecewise-linear approximation. The torus-doubling phenomenon was discovered by mutual coupling of four Chua's circuits in the paper [Zhong *et al*., 1998]. The authors [Zhong *et al*., 1998] also found that the attractors have a torus-like structure while the correct selection of resistors. The papers [Keuninckx, 2014; Keuninckx, 2015] present a two-transistor resistor-capacity phase shift oscillator to produce the chaotic behavior of the system. The feature of the proposed circuit is the absence of an inductor. Zhang et al. [2021; 2022] introduced the memristor into Chua's circuit. The possibility of generating multiscroll attractors by tuning the memristor internal parameters was demonstrated. Similar approach was used in the papers [Marco *et al*., 2022; Escudero *et al*., 2023]. In [Marco *et al*., 2022], Chua's circuit with a real non-volatile memristor that obeyed the Stanford model was considered, and in [Escudero *et al*., 2023] it was successfully integrated into the real device. Besides, two novel five-element chaotic circuits were designed by the current-controlled memristor in [Wang *et al*., 2023]. Rocha and Medrano-T [Rocha & Medrano-T, 2022] considered Chua's circuit with nonlinearity based on the exponential hyperbolic characteristics of semiconductors.

In addition to the above methods, strange attractors can be generated based on the experimental data set. In [Kennedy, 1994], based on experimental observations, the mathematical model of a bipolar junction transistor was proposed to simulate chaotic dynamics in the Colpitts oscillator. As stated in [Petrzela, 2016], a chaos can also be observed in state-variable filters. In addition to electrical circuits, strange attractors have been observed in mechanical and biological systems. So, Illing *et al.* [2012a] reduced the equations of motion of the Malkus water wheel to the Lorenz system. Based on experimental data, they determined the inclination angle, viscous damping rate, and total mass flux at which chaotic dynamics are achieved. The obtained results were further verified by an adaptive observer and an extended Kalman filter [Illing, 2012b]. Based on the observation data, a system of partial differential equations [Medvinsky *et al.*, 2002] was proposed to describe the aquatic ecosystem. This system exhibits chaotic behavior under the parameters given in [Medvinsky *et al.*, 2002; Kramer & Bollt, 2013]. Another example is the Hindmarsh-Rose neuron model in which chaotic dynamics can occur. In [Ma *et. al*; 2022], rotation control of the Hindmarsh-Rose was proposed for adjusting the offset of the neurons. Based on the obtained results, it was concluded that strange attractors can be rotated by a given angle without changing the phase space and LEs. Also, methods are being developed for reconstructing strange attractors from data using ordinary least squares [Karimov *et al.*, 2023] or the least squares method [Aguilar-Ibanez *et al.*, 2025]. Finally, some new aspects of different types of attractors creation [Danca *et al*., 2021; Qu *et al*., 2025] and investigation [Wang *et al*., 2023; Zhang *et al*., 2024] can be noted.

Generally, a strange attractor is considered a tool for image encryption problems [Wu *et al*., 2015; Wu *et al*., 2018; Niyat & Moattar, 2020]. However, generated strange chaotic attractors may be used to deliberately induce chaos in the dynamics of technical systems, thereby enabling novel ways of controlling their behavior.

For example, in [Doroshin, 2015; Doroshin, 2020] Wang-Sun and Chen-Lee chaotic attractors were initiated by the reaction wheels. The paper [Doroshin, 2018] developed this idea for the problem of transition from the initial zone if phase space to the desired one. We expanded this idea further and solved the chaotic reorientation problem using the differential evolution algorithm [Doroshin & Elisov, 2024].

This paper presents an applied case in which chaotic attractors offer a distinct approach to controlling the angular motion of spacecraft. Chaotic reorientation of spacecraft can be used as backup strategies for angular motion control. For example, in emergency scenarios where actuators are unable to execute standard reorientation maneuvers. Notably, chaos generated in the angular velocity space results in even greater complexity in the orientation angles. Consequently, by constructing compact chaotic attractors in angular velocity space, one can achieve nearly any orientation angle of spacecraft. Thus, energy-efficient chaotic regimes in angular velocity yield effective means for attaining arbitrary angles of spacecraft attitude.

Inspired by Sprott's studies [Sprott, 1993; Elhadj & Sprott, 2013], we propose two approaches for generating dynamical systems with chaotic attractors. The first one is similar to Sprott's approach and is named by the direct one. It is based on the searching of the coefficients of the nonlinear ODE system, and Lyapunov exponents (LE) are calculated using Benettin's algorithm [Benettin *et al.*, 1980; Benettin *et al.*, 1980]. Unlike Sprott, we use an optimization algorithm to generate strange attractors instead of randomly choosing coefficients. The second one is based on the controlled spacecraft attitude dynamics and it named by indirect approach. As shown in the papers [Doroshin, 2015; Doroshin, 2018; Doroshin, 2020], chaotic dynamics in spacecraft attitude can be created by a rotor electric engine and a jet engine. The indirect approach is based on searching for coefficients in the reaction wheel assembly control laws that satisfy the LE requirements. The main tool for searching dynamical systems with chaotic attractors is the differential evolution algorithm [Storn & Price, 1997].

The paper is organized as follows. In Section 2, the basic concepts of the two approaches are presented in detail. In Section 3, examples of chaotic attractors with analysis are given. The conclusions are drawn in Section 4.

2. Preliminaries

The current section is divided into two subsections. The first subsection describes the direct approach for synthesizing strange chaotic attractors. This approach synthesizes strange chaotic attractors, including those found in the Sprott system [Elhadj & Sprott, 2013], the Thomas attractor [Thomas, 1999], and the generalized Sprott system extended to higher dimensions. The second subsection describes the indirect approach for synthesizing strange chaotic attractors. It is based on the relationship between the dynamics of spacecraft angular motion and Sprott's system [Elhadj & Sprott, 2013].

2.1. *Direct approach*

As in [Sprott, 1993; Sprott, 2000], the main idea of the direct approach is to search for dynamical system coefficients which satisfy the required conditions of LEs. Let us consider the nonlinear ODE system proposed in [Elhadj & Sprott, 2013]:

$$\begin{cases} \dot{x} = a_0 + a_1 x + a_2 y + a_3 z + a_4 x^2 + a_5 y^2 + a_6 z^2 + a_7 xy + a_8 xz + a_9 yz, \\ \dot{y} = b_0 + b_1 x + b_2 y + b_3 z + b_4 x^2 + b_5 y^2 + b_6 z^2 + b_7 xy + b_8 xz + b_9 yz, \\ \dot{z} = c_0 + c_1 x + c_2 y + c_3 z + c_4 x^2 + c_5 y^2 + c_6 z^2 + c_7 xy + c_8 xz + c_9 yz, \end{cases} \tag{1}$$

where a_i, b_i, c_i are constant coefficients, and x, y, and z are the system state.

As well-known, 3D dynamical systems with chaotic behavior must have positive, null, and negative LEs:

$$\lambda_1 > 0, \tag{2}$$

$$\lambda_2 \approx 0, \tag{3}$$

$$\lambda_3 < 0. \tag{4}$$

An approach for assessing LEs is Benettin's algorithm [Benettin *et al*., 1980; Benettin *et al*., 1980]. For this approach, we need to introduce an additional system of ODEs in perturbations, which for Eq. (1) will take the form:

$$\begin{cases} \dot{\tilde{x}} = a_1\tilde{x} + a_2\tilde{y} + a_3\tilde{z} + 2a_4x\tilde{x} + 2a_5y\tilde{y} + 2a_6z\tilde{z} + a_7\left(\tilde{x}y + x\tilde{y}\right) + a_8\left(\tilde{x}z + x\tilde{z}\right) + a_9\left(\tilde{y}z + y\tilde{z}\right), \\ \dot{\tilde{y}} = b_1\tilde{x} + b_2\tilde{y} + b_3\tilde{z} + 2b_4x\tilde{x} + 2b_5y\tilde{y} + 2b_6z\tilde{z} + b_7\left(\tilde{x}y + x\tilde{y}\right) + b_8\left(\tilde{x}z + x\tilde{z}\right) + b_9\left(\tilde{y}z + y\tilde{z}\right), \\ \dot{\tilde{z}} = c_1\tilde{x} + c_2\tilde{y} + c_3\tilde{z} + 2c_4x\tilde{x} + 2c_5y\tilde{y} + 2c_6z\tilde{z} + c_7\left(\tilde{x}y + x\tilde{y}\right) + c_8\left(\tilde{x}z + x\tilde{z}\right) + c_9\left(\tilde{y}z + y\tilde{z}\right), \end{cases} \tag{5}$$

where $\tilde{x}$, $\tilde{y}$, and $\tilde{z}$ are small perturbations.

Since the considered system (1) has the three variables, the number of systems (5) is also will be three. Then, we simultaneously solve Eq. (1) and Eq. (5) for some initial conditions for $x(t_0)$, $y(t_0)$, $z(t_0)$, and $\left[\tilde{\mathbf{x}}(t_0) \quad \tilde{\mathbf{y}}(t_0) \quad \tilde{\mathbf{z}}(t_0)\right] = \mathrm{diag}(1 \quad 1 \quad 1)$. In accordance with [Benettin *et al*., 1980; Benettin *et al*., 1980], LEs are calculated on each integration step by the following relation:

$$\mathrm{LCE} = \frac{\mathbf{S}_{k+1}}{t_k}, \tag{6}$$

$$\mathbf{S}_{k+1} = \mathbf{S}_k + \ln\left(\mathbf{R}_{ii}\right), \tag{7}$$

$$\mathbf{S}(t_0) = \begin{bmatrix}0 & 0 & 0\end{bmatrix}^{\mathrm{T}}. \tag{8}$$

Here t_k is the current integration time; $\mathbf{R}_{ii}$ is the diagonal elements of the upper triangular matrix $\mathbf{R}$.

The upper triangular matrix $\mathbf{R}$ is the result of the QR decomposition of the result matrix $\mathbf{A}$:

$$\mathbf{A} = \mathbf{QR}, \tag{9}$$

$$\mathbf{A} = \begin{bmatrix} \tilde{x}'_{1k} & \tilde{y}'_{1k} & \tilde{z}'_{1k} \\ \tilde{x}'_{2k} & \tilde{y}'_{2k} & \tilde{z}'_{2k} \\ \tilde{x}'_{3k} & \tilde{y}'_{3k} & \tilde{z}'_{3k} \end{bmatrix}, \tag{10}$$

where $\mathbf{Q}$ is the orthonormal matrix, $\tilde{x}'_i$, $\tilde{y}'_i$, $\tilde{z}'_i$ are the integration results of Eq. (5).

To increase the numerical stability of QR decomposition, Householder transformation is used instead of the classical Gram-Schmidt process. After calculating the LEs at the current iteration k, perturbations $\tilde{\mathbf{x}}$, $\tilde{\mathbf{y}}$, $\tilde{\mathbf{z}}$ are reassigned by the following relation:

$$\begin{bmatrix} \tilde{x}_{1k+1} & \tilde{y}_{1k+1} & \tilde{z}_{1k+1} \\ \tilde{x}_{2k+1} & \tilde{y}_{2k+1} & \tilde{z}_{2k+1} \\ \tilde{x}_{3k+1} & \tilde{y}_{3k+1} & \tilde{z}_{3k+1} \end{bmatrix} = \mathbf{Q}. \tag{11}$$

Furthermore, a dynamical system exhibiting a strange attractor can be generated with a desired fractal dimension. The dimension of an attractor (in three dimensions) is calculated by the relation [Kaplan & Yorke, 1979]:

$$D_{KY} = 2 + \frac{\lambda_1 + \lambda_2}{\left|\lambda_3\right|} \tag{12}$$

Search for coefficients a_i, b_i, and c_i is carried out until conditions (2)-(4) are met. These coefficients can be found by randomly choosing [Sprott, 1993; Sprott, 2000] or using an optimization algorithm. For an optimization algorithm, the goal function must be introduced. Since the spacecraft attitude dynamics is considered in this paper, it is of interest to synthesize a strange attractor with minimum volume in the phase space with variables x, y, and z. Thus, we introduce the following goal function:

$$\Phi = \left(3 - YN_1 - YN_2 - YN_3\right)W_1 + \left\{\max\left(\left|x(t)\right|\right) + \max\left(\left|y(t)\right|\right) + \max\left(\left|z(t)\right|\right)\right\}W_2 + \left(D_{KY\,des} - D_{KY}\right)W_3 \to \min, \quad (13)$$

where W_i is the weight coefficient; YN_i is the binary value (YN_i = 1 or 0), reflecting the fulfillment of conditions (2)-(4), respectively; $D_{KY\,des}$ is the desired Kaplan-Yorke dimension.

The main advantage of this approach is the flexible configuration of the right-hand side of Eq. (1). In addition, the right-hand side of Eq. (1) may differ from the given one and includes another nonlinear term. As an example, we can consider the Thomas-like attractor [Thomas, 1999; Li & Sprott, 2017]:

$$\begin{cases} \dot{x} = a_0 + a_1 x + a_2 \sin\left(a_3 y\right), \\ \dot{y} = b_0 + b_1 y + b_2 \sin\left(b_3 z\right), \\ \dot{z} = c_0 + c_1 z + c_2 \sin\left(c_3 x\right), \end{cases} \quad (14)$$

The system of ODEs in perturbations has the following view:

$$\begin{cases} \dot{\tilde{x}} = a_1 \tilde{x} + a_2 a_3 \tilde{y} \cos\left(a_3 y\right), \\ \dot{\tilde{y}} = b_1 \tilde{y} + b_2 b_3 \tilde{z} \cos\left(b_3 z\right), \\ \dot{\tilde{z}} = c_1 \tilde{z} + c_2 c_3 \tilde{x} \cos\left(c_3 x\right), \end{cases} \quad (15)$$

Moreover, system (1) can be expanded by an additional dimension for generating hyperchaotic attractors. Let us rewrite Eq. (1) and Eq. (5) in the matrix form:

$$\dot{\mathbf{f}} = \mathbf{B}\mathbf{f}, \quad (16)$$

$$\dot{\tilde{\mathbf{f}}} = \mathbf{B}\tilde{\mathbf{f}}, \quad (17)$$

where $\mathbf{f}$ is the vector of phase variables; $\tilde{\mathbf{f}}$ is the vector of small perturbations; $\mathbf{B}$ is the matrix of coefficients.

For the 4D dynamical system, vectors $\mathbf{f}$, $\tilde{\mathbf{f}}$ and matrix $\mathbf{B}$ have the following form:

$$\mathbf{f} = \left[1, \quad x, \quad y, \quad z, \quad w, \quad x^2, \quad y^2, \quad z^2, \quad w^2, \quad xy, \quad xz, \quad xw, \quad yz, \quad yw, \quad zw\right]^{\mathrm{T}}, \quad (18)$$

$$\mathbf{B} = \begin{bmatrix} a_0 & a_1 & a_2 & a_3 & a_4 & a_5 & a_6 & a_7 & a_8 & a_9 & a_{10} & a_{11} & a_{12} & a_{13} & a_{14} \\ b_0 & b_1 & b_2 & b_3 & b_4 & b_5 & b_6 & b_7 & b_8 & b_9 & b_{10} & b_{11} & b_{12} & b_{13} & b_{14} \\ c_0 & c_1 & c_2 & c_3 & c_4 & c_5 & c_6 & c_7 & c_8 & c_9 & c_{10} & c_{11} & c_{12} & c_{13} & c_{14} \\ d_0 & d_1 & d_2 & d_3 & d_4 & d_5 & d_6 & d_7 & d_8 & d_9 & d_{10} & d_{11} & d_{12} & d_{13} & d_{14} \end{bmatrix}, \quad (19)$$

$$\tilde{\mathbf{f}} = \left[0, \quad \tilde{x}, \quad \tilde{y}, \quad \tilde{z}, \quad \tilde{w}, \quad 2x\tilde{x}, \quad 2y\tilde{y}, \quad 2z\tilde{z}, \quad 2w\tilde{w}, \quad \tilde{x}y + x\tilde{y}, \quad \tilde{x}z + x\tilde{z}, \quad \tilde{x}w + x\tilde{w}, \quad \tilde{y}z + y\tilde{z}, \quad \tilde{y}w + y\tilde{w}, \quad \tilde{z}w + z\tilde{w}\right]^{\mathrm{T}}. \quad (20)$$

To generate a hyperchaotic attractor, Eq. (13) must be rewritten in the following form:

$$\Phi = 4 - YN_1 - YN_2 - YN_3 - YN_4 \to \min, \quad (21)$$

where YN_i is the binary value which reflects the following conditions:

$$\lambda_1, > 0, \tag{22}$$

$$\lambda_2 > 0, \tag{23}$$

$$\lambda_3 \approx 0, \tag{24}$$

$$\lambda_4 < 0. \tag{25}$$

As mentioned above, strange attractors can be used for encryption [Wu *et al*., 2015; Wu *et al*., 2018; Niyat & Moattar, 2020] or spacecraft reorientation problems [Doroshin, 2015; Doroshin, 2020; Doroshin & Elisov, 2024]. However, the direct approach is a general one that cannot always be applied to specific problems (in our case, in the spacecraft reorientation problem). In this regard, we also propose an indirect approach that can generate strange attractors related with a specific application problem.

2.2. *Indirect approach*

The practical aspects of using dynamical chaos themselves become natural sources of approaches for generating chaotic dynamical systems. In other words, if we have a physical system described by a nonlinear equation system, we can attempt to initiate a strange attractor by varying its coefficients.

One example of such a situation could be the dynamics of a spacecraft, when we can initiate strange chaotic attractors in its motion. Below, we consider this particular problem of strange chaotic attractors generation in the dynamics of spacecraft, which will represent a basic example for the indirect approach in general.

According to [Doroshin, 2015], the spacecraft attitude dynamics will take on chaotic behavior if the chosen control coefficients correspond to a particular strange attractor (Wang-Sun, Newtow-Leipnik etc.). The search for control coefficients that cause the chaotic behavior was conducted using gradient descent [Doroshin, 2015].

Notably, the approach in this form will not always generate new strange attractors because it depends on the convergence of the solution. In other words, the obtained coefficients can correspond to well-known strange attractors [Doroshin, 2015], generate a new one [Doroshin, 2016], or generate a nonchaotic attractor. Thus, prerequisites for creating an indirect approach appeared. Then, we made some modifications to the indirect approach in our study. Based on the papers [Doroshin, 2014; Doroshin, 2015; Doroshin, 2018], let us consider the attitude dynamics of spacecraft equipped with a reaction wheel assembly (RWA). Spacecraft with RWA (Fig. 1) represents the so-called multirotor mechanical system (the multispin spacecraft).

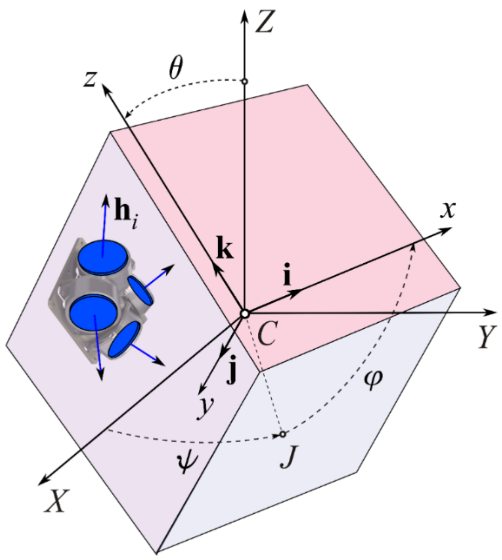

Fig. 1. Mechanical structure of the spacecraft with RWA.

In Fig. 1, the main coordinate systems are locally used: C_{XYZ} is the inertial frame, C_{xyz} is the frame connected to the main body of the spacecraft, where C is the center of mass of the system, and connected axes x, y, and z correspond to the central principal axes of the mechanical system. Notably, the coordinate frames C_{XYZ} and C_{xyz} (Fig. 1) are simply geometric; they are used locally and are not related in any way to the parameters of the dynamical system (1).

The attitude dynamics of this spacecraft can be described by the law of the angular momentum changing:

$$\begin{aligned} &\frac{d\mathbf{K}}{dt} + \boldsymbol{\omega} \times \mathbf{K} = \mathbf{M}^e, \\ &\mathbf{K} = \mathbf{K}_{rb} + \mathbf{H} \end{aligned} \tag{26}$$

where $\mathbf{K}$ is the angular momentum vector of the complete mechanical system; $\boldsymbol{\omega}$ is the angular velocity vector of the main body of the spacecraft; $\mathbf{K}_{rb}$ is the angular momentum of the main rigid body of the spacecraft together with the internal immovable ("freezed") rotors of the RWA; $\mathbf{H}$ is the relative angular momentum of the RWA, which is created by the rotations of the rotors relative to the main rigid body; $\mathbf{M}^e$ is the vector of the external torques acting on the system.

The relative angular momentum $\mathbf{H}$ of the RWA is formed as a sum of the separate angular momentum of each rotor from the assembly:

$$\mathbf{H} = \sum_{k=1}^{N} \mathbf{h}_k; \quad \mathbf{h}_k = I_k \sigma_k \mathbf{e}_k \tag{27}$$

where N is the number of rotors in RWA, I_k is the inertia moment of the k-th rotor, σ_k is the angular velocity of the k-th rotor relative to the main rigid body, and $\mathbf{e}_k$ is the unit vector of the direction of the k-th rotor rotation given in the connected frame C_{xyz}.

In the scalar form, Eq. (26) can be written in projections onto the axes of the connected frame C_{xyz}:

$$\begin{cases} A\dot{p} + \dot{H}_x + (C-B)qr + \left[qH_z - rH_y\right] = M_x^e, \\ B\dot{q} + \dot{H}_y + (A-C)rp + \left[rH_x - pH_z\right] = M_y^e, \\ C\dot{r} + \dot{H}_z + (B-A)pq + \left[pH_y - qH_x\right] = M_z^e, \end{cases} \tag{28}$$

where A, B, and C are the general moments of inertia of the main body with immovable "freezed" rotors of the RWA; p, q, and r are components of the angular velocity of the main body $\boldsymbol{\omega}$ in projections onto connected axes C_{xyz}. The components of the relative angular momentum of the RWA have the following form:

$$H_x = \sum_{k=1}^{N} c_{xk} I_k \sigma_k; \quad H_y = \sum_{k=1}^{N} c_{yk} I_k \sigma_k; \quad H_z = \sum_{k=1}^{N} c_{zk} I_k \sigma_k, \tag{29}$$

where $c_{xk} = \mathbf{e}_k \cdot \mathbf{i}$; $c_{yk} = \mathbf{e}_k \cdot \mathbf{j}$; $c_{zk} = \mathbf{e}_k \cdot \mathbf{k}$ are the constant directional cosines of the axis of rotation of the k-th rotor ($\mathbf{i}$, $\mathbf{j}$, and $\mathbf{k}$ are the unit vectors of the connected frame C_{xyz}).

The equation of the relative rotation of the k-th rotor follows from the law of the angular momentum changing:

$$I_k\left(c_{xk}\dot{p} + c_{yk}\dot{q} + c_{zk}\dot{r} + \dot{\sigma}_k\right) = M_k^{control}, \ k = 1...N \tag{30}$$

Here $M_k^{control}$ is the internal torque acting on the k-th rotor from the side of the control system of the spacecraft. The torques $M_k^{control}$ $(k = 1...N)$ form the programed vector $\mathbf{H}$ of the relative angular momentum of RWA by the programed change in the angular velocity of the relative rotation σ_k. The torques $M_k^{control}$ $(k = 1...N)$ are created using an electric motor mounted in the main body, which is controlled by the control system of the spacecraft.

Let us consider the case when the RWA relative angular momentum $\mathbf{H}$ is formed by the control system in the following form [Doroshin, 2015; Doroshin, 2020]:

$$H_x(t)=\alpha_p p+\alpha_0;\ H_y(t)=\beta_q q+\beta_0;\ H_z(t)=\gamma_r r+\gamma_0, \tag{31}$$

where $\{\alpha_0, \alpha_p, \beta_0, \beta_q, \gamma_0, \gamma_r\}$ are the predefined control parameters.

Additionally, the control system may create the external torques in the following form [Doroshin, 2018; Doroshin & Elisov, 2024]:

$$\begin{cases} M_x^e = m_x + \alpha_1 p, \\ M_y^e = m_y + \beta_1 q, \\ M_z^e = m_z + \gamma_1 r, \end{cases} \tag{32}$$

where m_x, m_y, m_z, α_1, β_1, γ_1 are also the predefined control parameters. These external torques can be formed by magnetic coils mounted in spacecraft and jet-rocket engines.

So, the chosen control laws (31) and (32) have twelve predefined parameters α_0, α_1, α_p, β_0, β_1, β_q, γ_0, γ_1, γ_r, m_x, m_y, m_z, which define the dynamical mode of the angular motion of the spacecraft. Our goal is to initiate and support a chaotic mode in attitude dynamics using the control vector **U**:

$$\mathbf{U}=\left[\alpha_0,\alpha_1,\alpha_p,m_x,\beta_0,\beta_1,\beta_q,m_y,\gamma_0,\gamma_1,\gamma_r,m_z\right]^T. \tag{33}$$

The relationship between Eq. (1) and Eq. (33) can be established using the following steps. First, we need to substitute Eq. (31) and Eq. (32) into Eq. (28). After these substitutions, system (1) can be considered the complete first-order system of differential equations relatively p, q, r. Second, we reassign the variables $p \leftrightarrow x$, $q \leftrightarrow y$, $r \leftrightarrow z$ and collect similar terms. Then, the following correspondences for parameters can be obtained [Doroshin, 2018]:

$$\begin{cases} a_0 = m_x\left(A+\alpha_p\right)^{-1},\ b_0 = m_y\left(B+\beta_q\right)^{-1},\ c_0 = m_z\left(C+\gamma_r\right)^{-1}, \\ a_1 = \alpha_1\left(A+\alpha_p\right)^{-1},\ b_1 = \gamma_0\left(B+\beta_q\right)^{-1},\ c_1 = -\beta_0\left(C+\gamma_r\right)^{-1}, \\ a_2 = -\gamma_0\left(A+\alpha_p\right)^{-1},\ b_2 = \beta_1\left(B+\beta_q\right)^{-1},\ c_2 = \alpha_0\left(C+\gamma_r\right)^{-1}, \\ a_3 = \beta_0\left(A+\alpha_p\right)^{-1},\ b_3 = -\alpha_0\left(B+\beta_q\right)^{-1},\ c_3 = \gamma_1\left(C+\gamma_r\right)^{-1}, \\ a_4 = a_5 = a_6 = b_4 = b_5 = b_6 = c_4 = c_5 = c_6 \equiv 0, \\ a_7 = b_7 \equiv 0,\ c_7 = \left(A-B-\beta_q+\alpha_p\right)\left(C+\gamma_r\right)^{-1}, \\ a_8 = c_8 \equiv 0,\ b_8 = \left(C-A-\alpha_p+\gamma_r\right)\left(B+\beta_q\right)^{-1}, \\ b_9 = c_9 \equiv 0,\ a_9 = \left(B-C-\gamma_r+\beta_q\right)\left(A+\alpha_p\right)^{-1}. \end{cases} \tag{34}$$

In previous studies [Doroshin, 2018; Doroshin, 2020; Doroshin & Elisov, 2024], the control vector **U** was calculated using the gradient descent method to meet the conditions (34) for predefined coefficients $\{a_i, b_i, c_i\}$ corresponding to the concrete type of strange attractor (e.g. to Newton-Leipnik type, or others).

In this study, we select the control vector **U** so that the coefficients a_i, b_i, and c_i obtained from Eq. (34) satisfy conditions (2)-(4). The goal function for the indirect approach can be similar to Eq. (13). However, the most interesting are the strange attractors that can be generated with minimal control **U**. Therefore, the goal function (13) is rewritten as:

$$\Phi=\left(3-YN_1-YN_2-YN_3\right)W_1+W_2\sum_{i=1}^{12}\left|U_i\right|\to \min, \tag{35}$$

The main advantage of the indirect approach is its applicability to specified problems, for example, for chaotic reorientation of spacecraft, since it is derived from its physics. Notably, the form of the control laws (31) and (32) does not produce the quadratic terms (x^2, y^2, and z^2) in Eq. (1). To obtain Eq. (1) with quadratic terms, we should choose some other forms of the control, but in the framework of research, this aspect is not so important.

3. Results

Let us divide this section of our paper into two subsections. The first subsection is devoted to the results obtained by the direct approach. It includes the results of the generation of strange attractors existing in Eq. (1) and Eq. (14), as well as the "optimal" strange attractors obtained from condition (13). Moreover, the obtained results also include the hyperchaotic attractors existing in Eq. (18)-(19). LEs, Kaplan-Yorke dimensions, and bifurcation diagrams are given for all the obtained attractors.

The second subsection presents the results of generating strange attractors by the indirect approach using Eq. (1), Eq. (13), Eq. (33) and Eq. (34). As in the first subsection, the analysis of the obtained strange attractors will also be provided.

The coefficients of Eq. (1) (for the direct method) and Eq. (34) (for the indirect method) are given in Appendix A. The initial conditions are also given in Appendix A.

Strange attractors with the desired Kaplan-Yorke dimension are presented in Appendix B. For these attractors, only the phase space and LEs are given without analysis. The initial conditions are similar to the presented strange attractors (see Table A1 in Appendix A).

3.1. *Generation of a strange attractor using direct approach*

The numerical calculations were performed using the MATLAB program for 3D systems. To improve the performance of calculations, higher-dimensional systems were modeled using the C language. The fourth order Runge-Kutta integration algorithm was performed to solve the considered differential equations. The integration step is set constant and equal to 0.001 s.

The population size N for the differential evolution algorithm is equal to the number of searched coefficients multiplied by 10. The mutation and crossover parameters are the same for all systems considered and are set to $F = 0.5$ and $P = 0.99$, respectively.

As mentioned above, the generation of strange attractors was conducted using the differential evolution algorithm. Due to the nature of the nonlinearity of Eq. (1) and Eq. (18), there is no single solution. Thus, the analysis is performed for one unoptimized and one optimized strange attractor.

It is important to define our terms "unoptimized" and "optimized" strange attractors. Our "unoptimized" strange attractors are strange attractors generated for weight coefficients $W_1 = 1$ and $W_2 = W_3 = 0$ in Eq. (13). Our "optimized" strange attractors are strange attractors generated with improved properties (e.g., minimum phase volume): in the case of the goal function (13) the weight coefficients are equal $W_1 = 100$, $W_2 = 1$, and $W_3 = 0$; and for the goal function (35) these values are $W_1 = 1000$ and $W_2 = 1$.

Firstly, let us consider system (1) including all nonzero 30 coefficients. Such systems can be called a "complete". The comparison of the unoptimized #1 and optimized #1 strange attractors is shown in Fig. 2. The unoptimized strange attractor #1 has a complex structure. On the other hand, the optimized strange attractor #1 has a simpler structure than the unoptimized one.

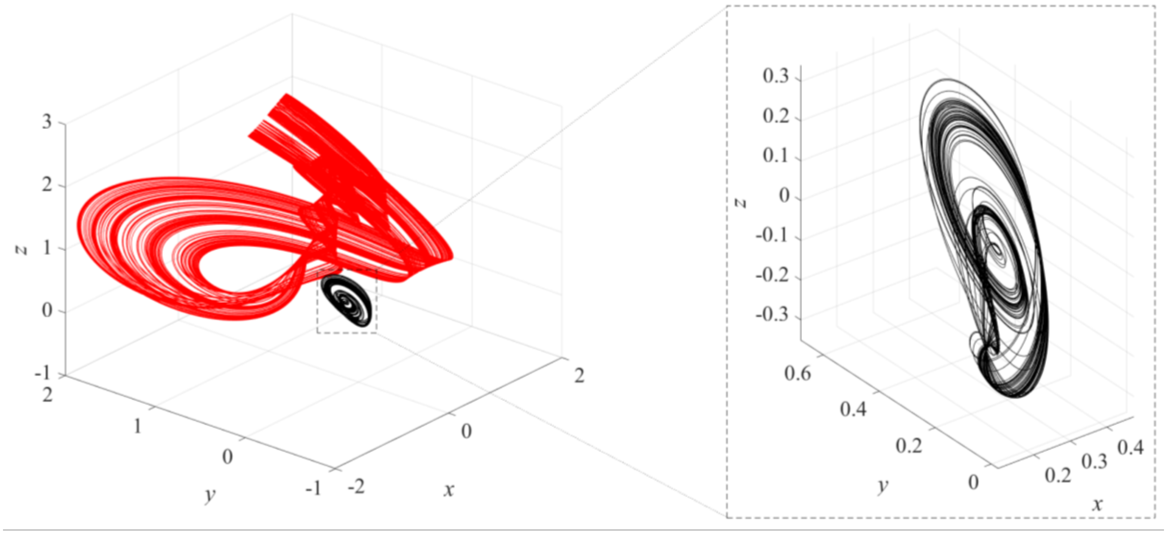

Fig. 2. Comparison between unoptimized #1 (red) and optimized #1 (black) strange attractors.

As shown in Fig. 3, both attractors have positive, zero, and negative LEs. Kaplan-Yorke dimension is 2.06 and 2.117 for the unoptimized #1 and optimized #1 attractors, respectively.

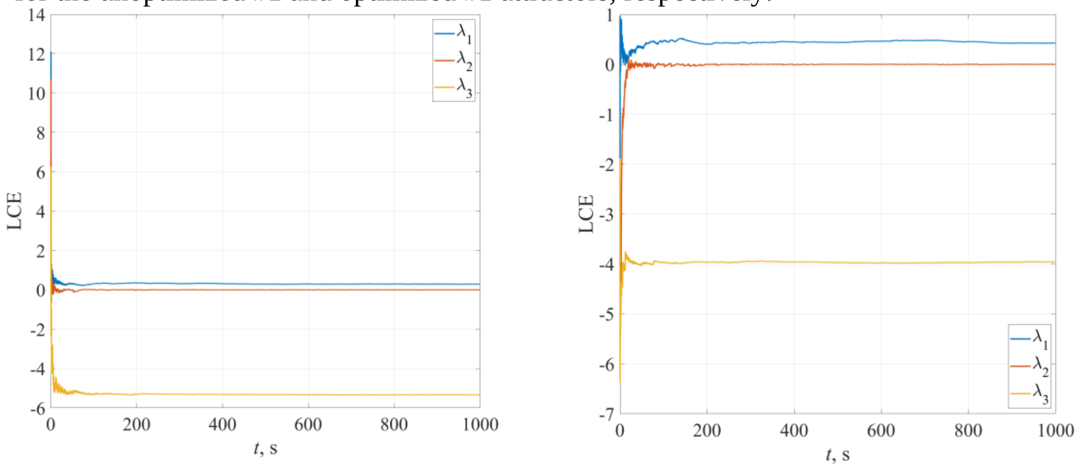

(a) Unoptimized strange attractor #1

(b) Optimized strange attractor #1

Fig. 3. LEs for the complete system.

It is important and interesting to analyze the parametric zones of the system chaotic behavior. For these purposes, the bifurcation diagrams for the system are calculated. All bifurcation diagrams correspond to equilibrium points for the dynamical variable $x(t)$ and their repetition cycles depending on the system coefficient values. As can be seen from the diagram (Fig. 4), the dynamical systems for the unoptimized #1 and optimized #1 strange attractors have different zones of the dynamical behavior relative to the coefficient a_0 (at all other fixed coefficients).

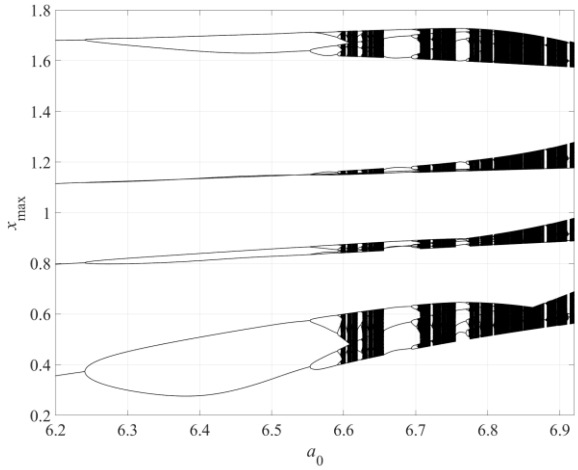

(a) 1D bifurcation diagram for unoptimized #1

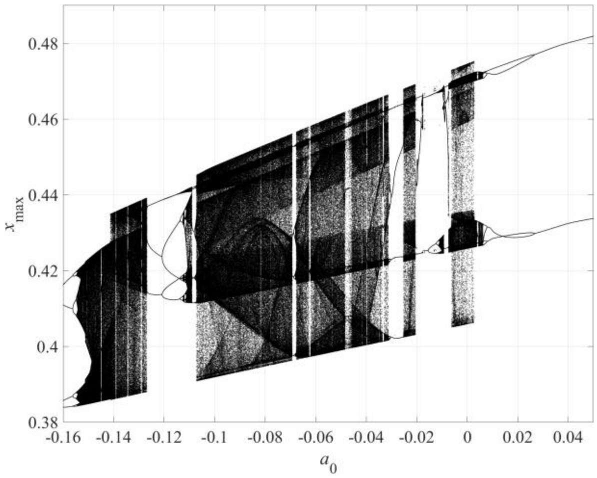

(b) 1D bifurcation diagram for optimized #1

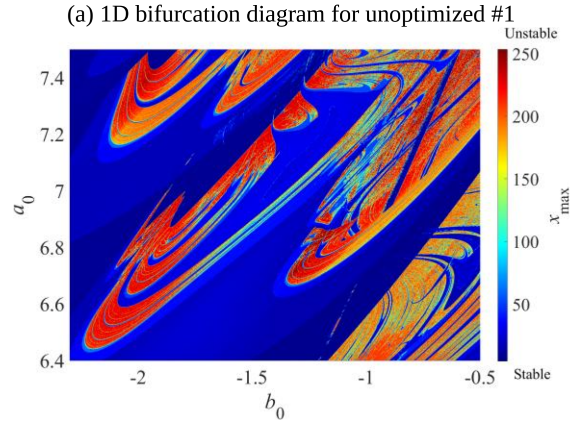

(c) 2D bifurcation diagram for unoptimized #1

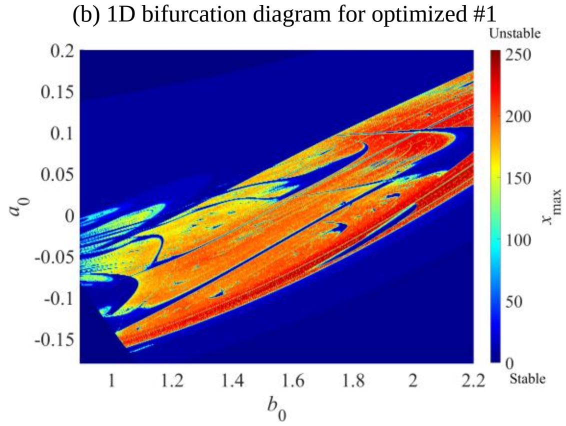

(d) 2D bifurcation diagram for optimized #1

Fig. 4. Bifurcation diagrams.

Notably, certain diagrams (Fig.4(c), Fig. 4(d), and some following ones) are rendered in two dimensions, wherein color encodes the respective levels of stability and instability within the dynamics, which delineate the thresholds between regular and chaotic behavior.

The chaotic behavior of an unoptimized strange attractor will retain its chaotic behavior on some intervals of the coefficient a_0 value, e.g. if $a_0 \in \{[6.59, 6.6], [6.61, 6.62], [6.63, 6.65], [6.71, 6.72], [6.73, 6.76], [6.78, 6.81]\}$, and also for other intervals alternating with intervals of regularity. Such alternations of the chaotic and regular intervals demonstrate the broad variability of the coefficient value allowing initialization of the chaotic attractor.

The same properties are actual for the optimized system. Other examples of optimized strange attractors for the complete system are shown in Fig. 5.

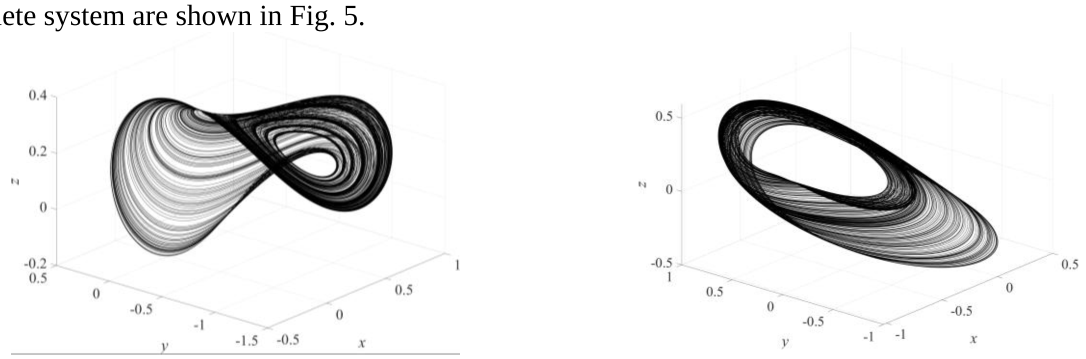

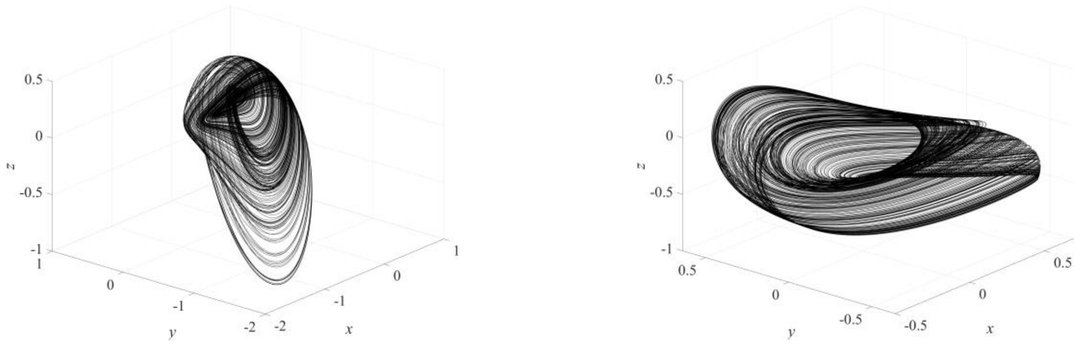

Fig. 5. Family of the complete system (1).

Secondly, it is important to synthesize the dynamical systems contained a strange attractor at a minimal number of nonlinear terms in Eq. (1). Let us consider the synthesis of dynamical systems with only one nonlinear term in each equation of system (1). Such systems can be called a “reduced system”. One of the possible examples of the reduced system is presented below as attractor #2. The strange attractor #2 for the reduced system is depicted in Fig. 6.

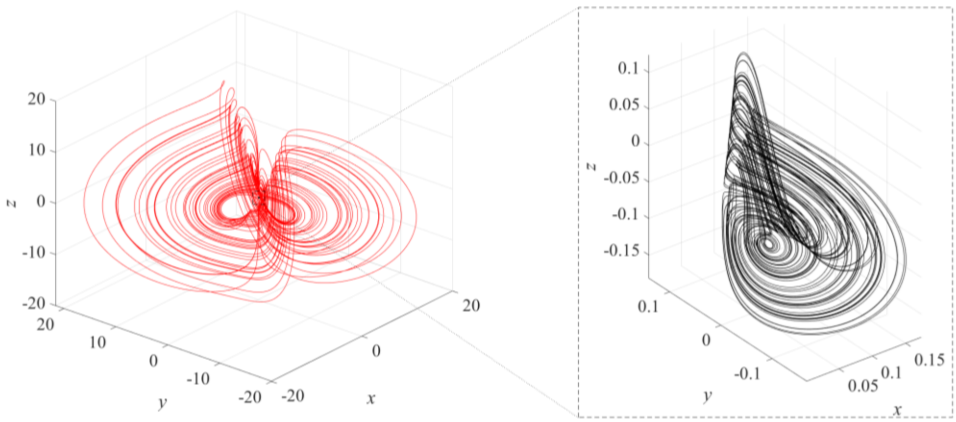

Fig. 6. Comparison between unoptimized #2 (red) and optimized #2 (black) strange attractors.

LEs for the unoptimized #2 and optimized #2 strange attractors are shown in Fig. 7. The Kaplan-Yorke dimension is equal 2.14 and 2.112 for unoptimized #2 and optimized #2 attractors, respectively.

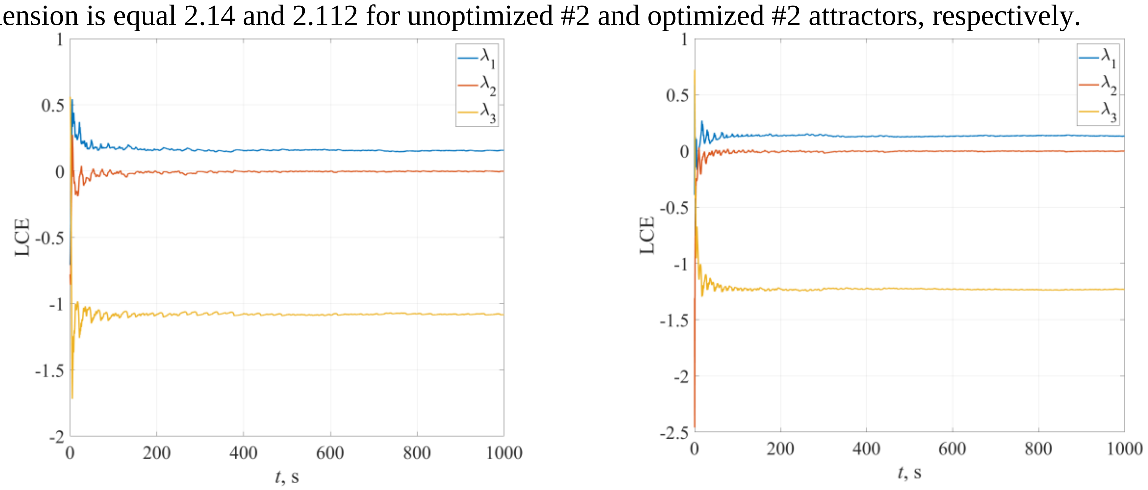

(a) Unoptimized strange attractor #2

(b) Optimized strange attractor #2

Fig. 7. LEs for the reduced system.

Bifurcation diagrams for unoptimized #2 and optimized #2 strange attractor are given at Fig. 8, whereas changing parameter was used for coefficient a_1.

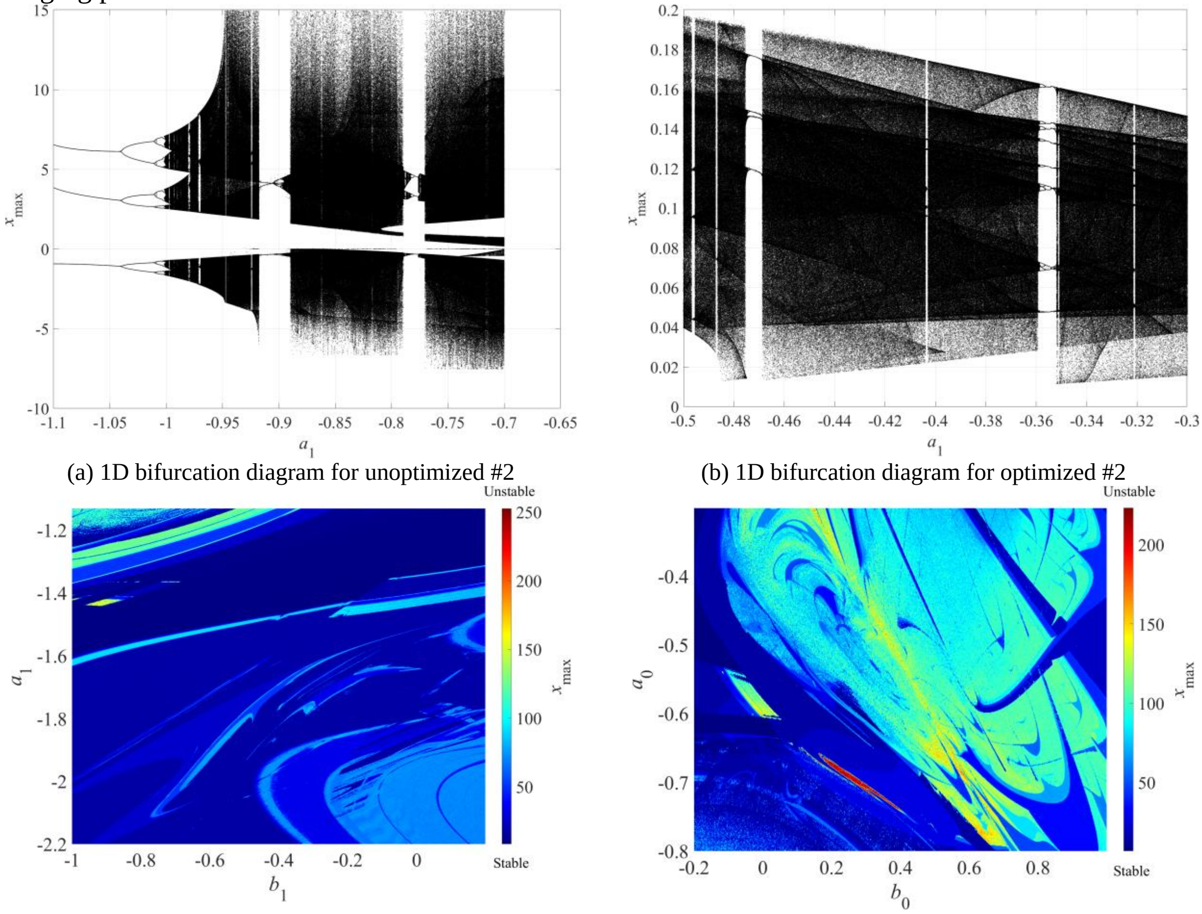

(a) 1D bifurcation diagram for unoptimized #2

(b) 1D bifurcation diagram for optimized #2

(c) 2D bifurcation diagram for unoptimized #2

(d) 2D bifurcation diagram for optimized #2

Fig. 8. Bifurcation diagrams.

In addition to the optimized strange attractor #2, some other examples of optimized strange attractors for the reduced system are presented in Fig. 9.

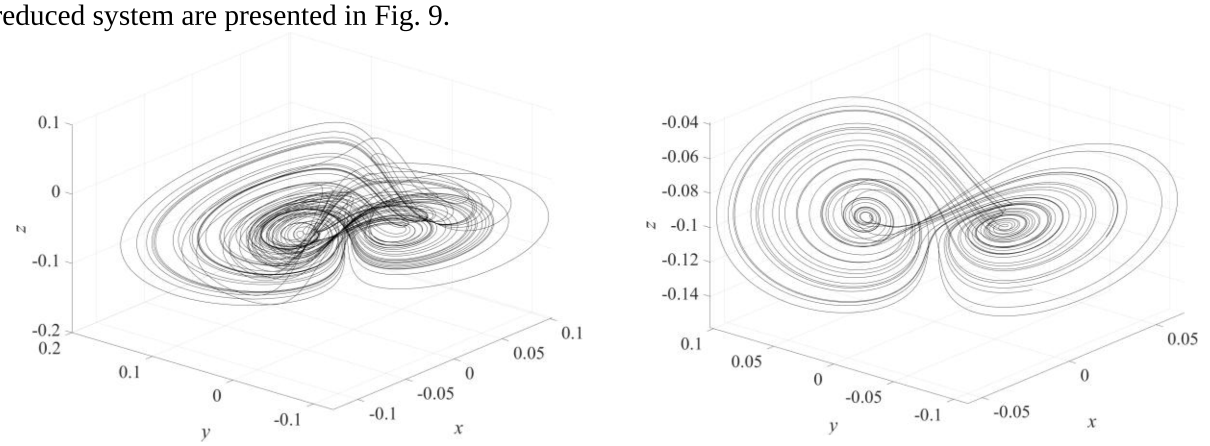

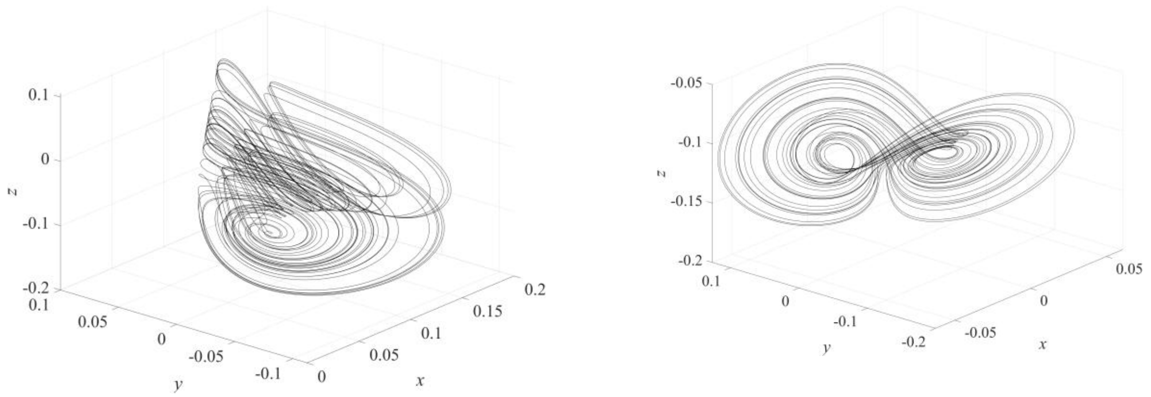

Fig. 9. Family of the reduced system (1).

Let us consider the case, which is based on Thomas-like attractors (18). This strange attractor is denoted as strange attractor #3. The strange attractor #3 is shown in Fig. 10.

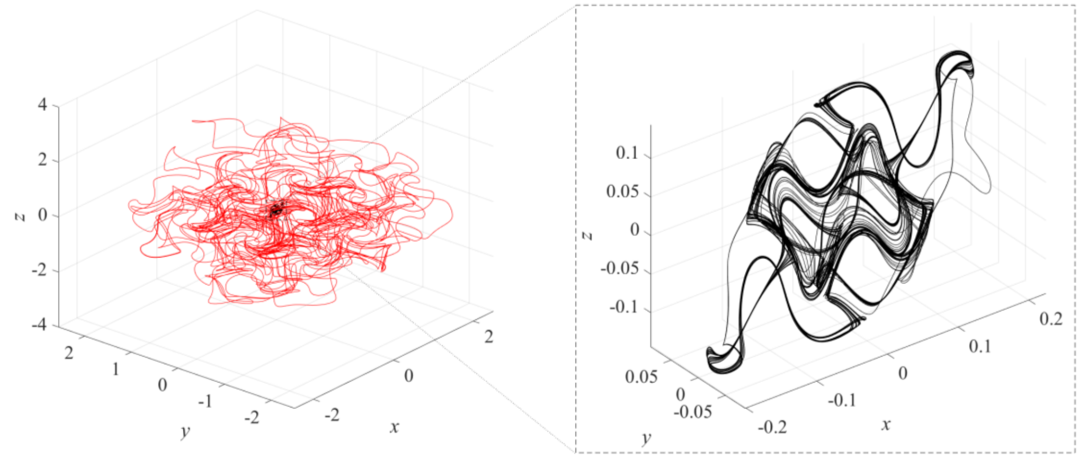

Fig. 10. Comparison between unoptimized #3 (red) and optimized #3 (black) strange attractors.

LEs for the unoptimized #3 and optimized #3 strange attractors are presented in Fig. 11. The Kaplan-Yorke dimension is equal to 2.574 and 2.047 for the unoptimized #3 and optimized #3 attractors, respectively.

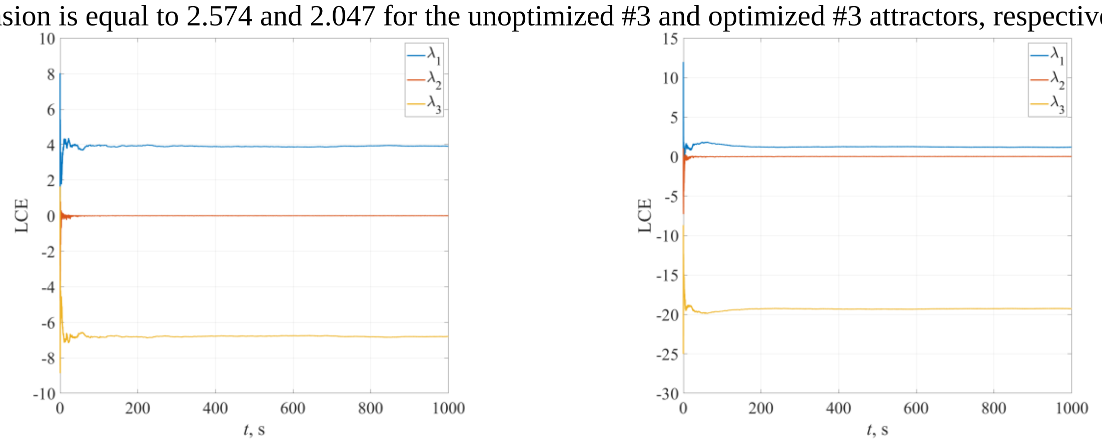

(a) Unoptimized strange attractor #3

(b) Optimized strange attractor #3

Fig. 11. LEs for Thomas-like attractor.

Bifurcation diagrams for unoptimized #3 and optimized #3 chaotic attractors are shown in Fig. 12. For the unoptimized #3 attractor, coefficients a_3, b_3, and c_3 changed when plotting the diagram. For the optimized #3 attractor, only the coefficient a_1 changed. 2D bifurcation diagrams for unoptimized #3 and optimized #3 chaotic attractors are not shown, as they are not informative.

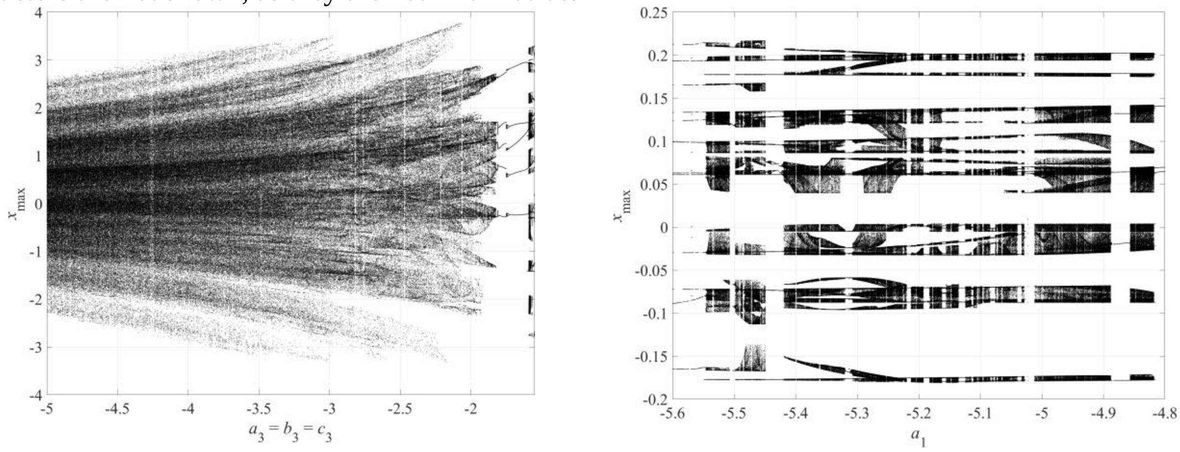

(a) 1D bifurcation diagram for unoptimized #3

(b) 1D bifurcation diagram for optimized #3

Fig. 12. Bifurcation diagrams.

Other examples of optimized strange attractors for the Thomas-like system are shown in Fig. 13.

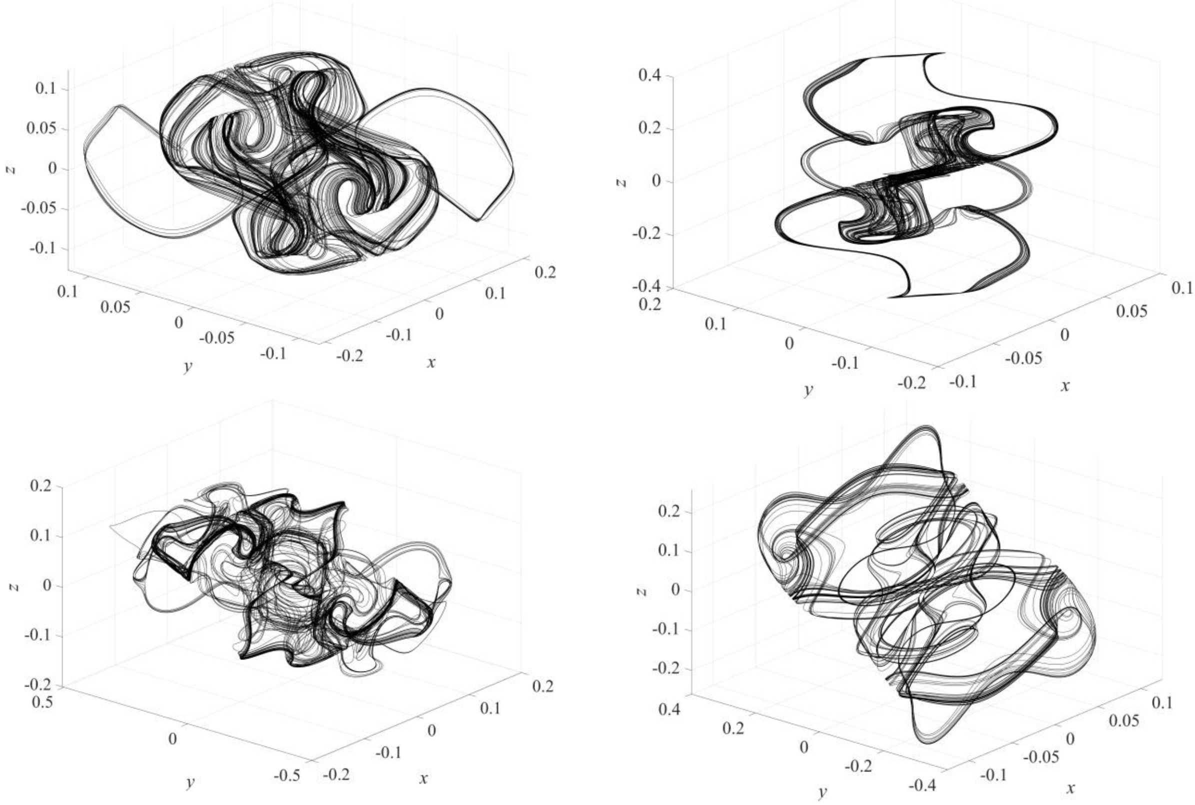

Fig. 13. Family of the Thomas-like attractor.

Finally, let us consider the case of the generation of hyperchaotic attractors. Generation of a hyperchaotic attractor is provided in two ways. The first one is based on the generated chaotic attractor (unoptimized #2 and optimized #2). In this case, the search for coefficients based on the obtained ones is performed in the neighborhood and for the additional variable *w*, in an arbitrary region, which satisfy the conditions (22)-(25). These attractors are denoted as hyper #1 and hyper #2.

The second way of generating hyperchaotic attractors is similar to the generation of chaotic attractors. However, the search for the coefficients of equation (17) must satisfy the conditions (22)-(25).

Notably, 2D bifurcation diagrams for these attractors are not provided due to lack of clarity. An example of generating a hyperchaotic attractor hyper #1 based on a unoptimized attractor #2 is shown in Fig. 14. The coefficients of this attractor are given in Table A8 in the Appendix.

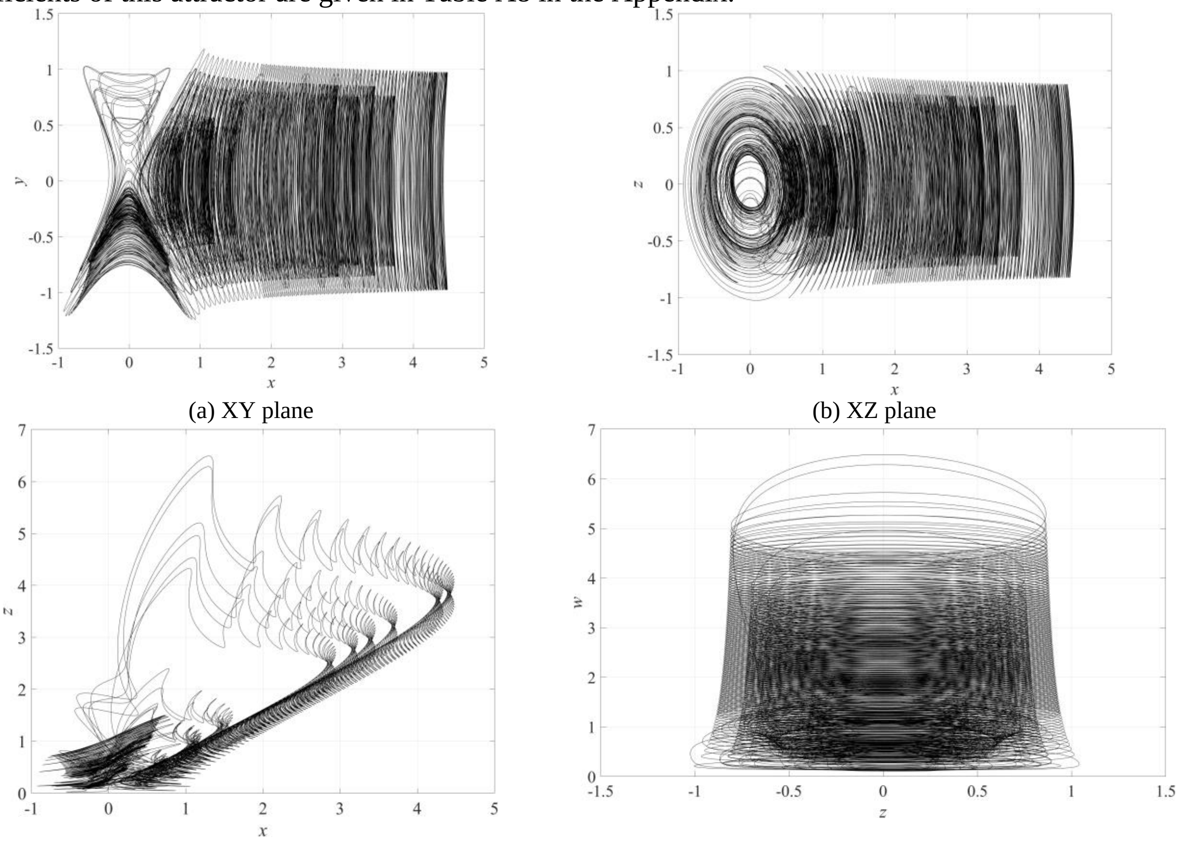

(a) XY plane (b) XZ plane

(c) XW plane (d) ZW plane

Fig. 14. Hyperchaotic strange attractor hyper #1.

The generated attractor has two positive, one zero, and one negative LEs (Fig. 15). The Kaplan-Yorke dimension is equal to 3.2523.

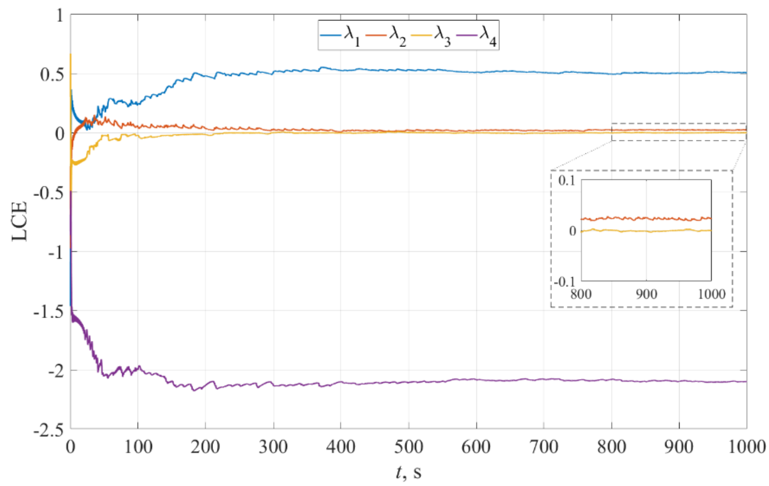

Fig. 15. LEs for hyperchaotic attractor hyper #1.

Bifurcation diagram for hyper #1 hyperchaotic attractor is shown in Fig. 16.

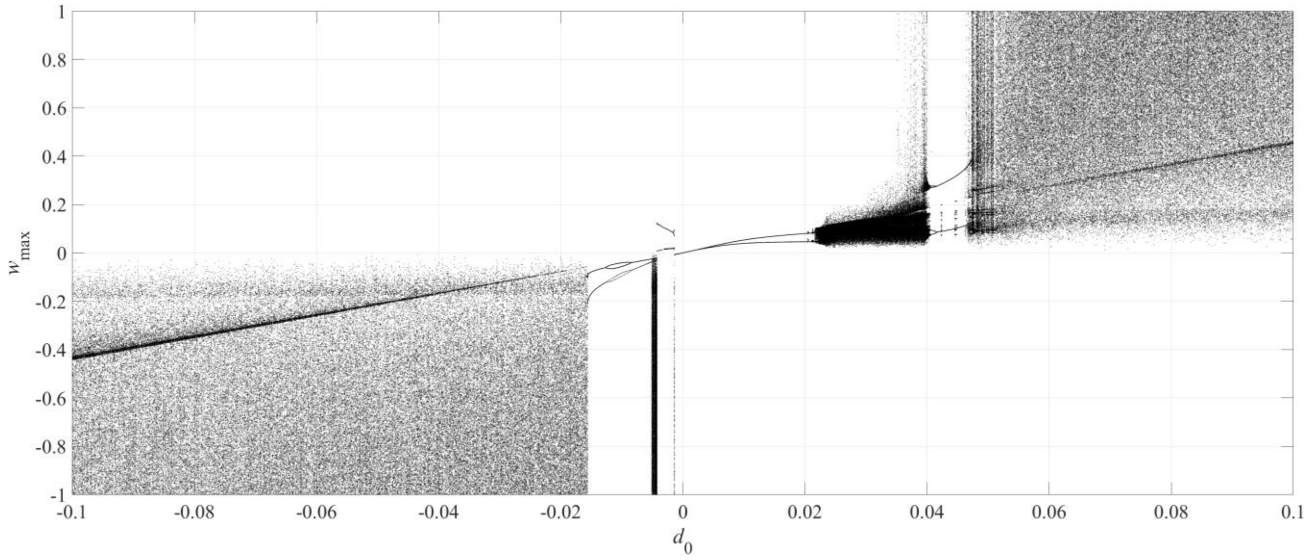

Fig. 16. Bifurcation diagram for hyperchaotic attractor hyper #1.

Next, Fig. 17 shows the generated hyperchaotic attractor hyper #2 based on the optimized attractor #2. Unlike attractor hyper #1, attractor hyper #2 has a more complex structure. The coefficients of the attractor hyper #2 are also given in Table A8 in the Appendix.

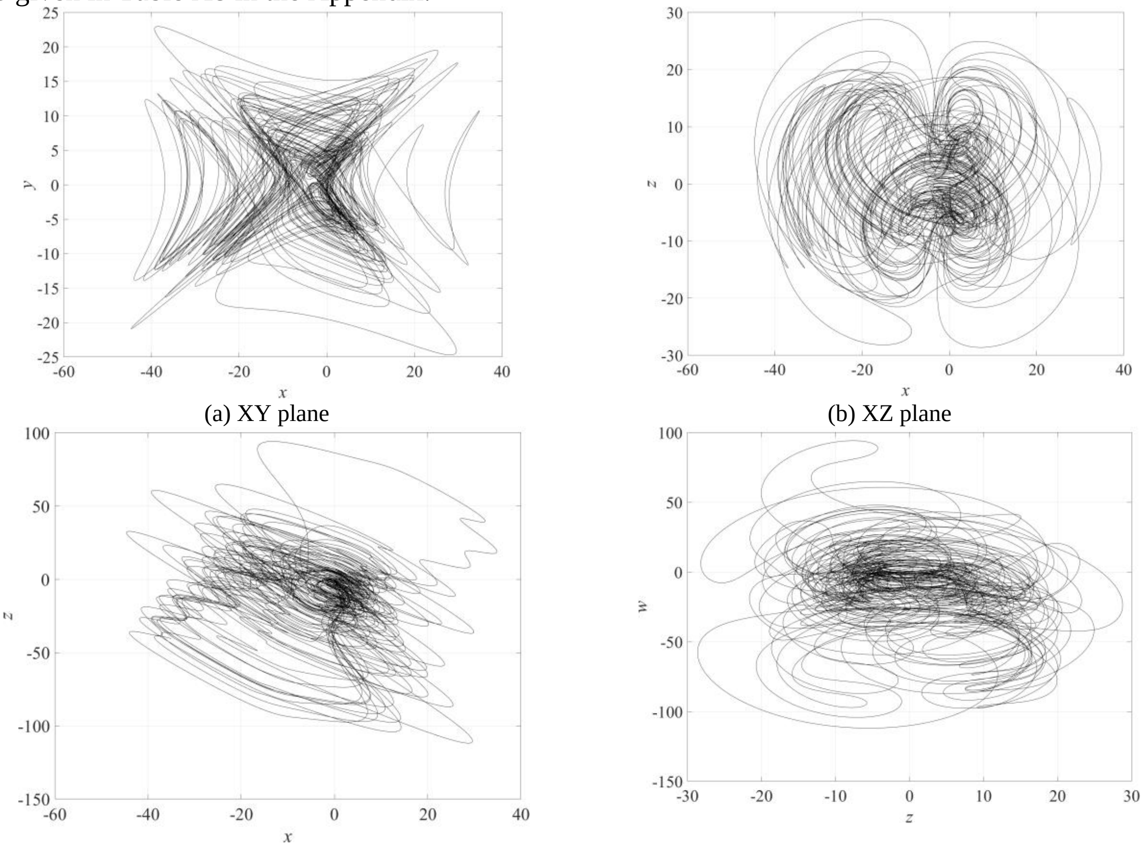

(a) XY plane (b) XZ plane

(c) XW plane (d) ZW plane

Fig. 17. Hyperchaotic strange attractor hyper #2.

As in the previous case, the generated attractor has two positive, one zero and one negative LEs (Fig. 18). The Kaplan-Yorke dimension is equal to 3.0909.

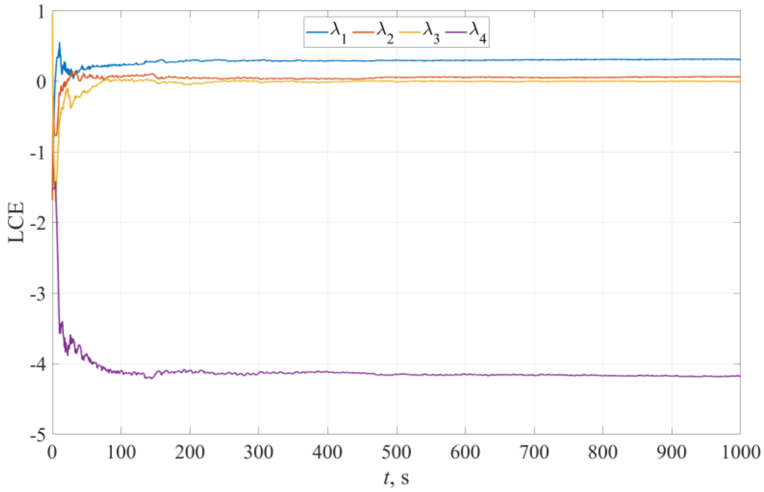

Fig. 18. LEs for hyperchaotic attractor hyper #2.

Bifurcation diagram for hyperchaotic attractor hyper #2 is shown in Fig. 19.

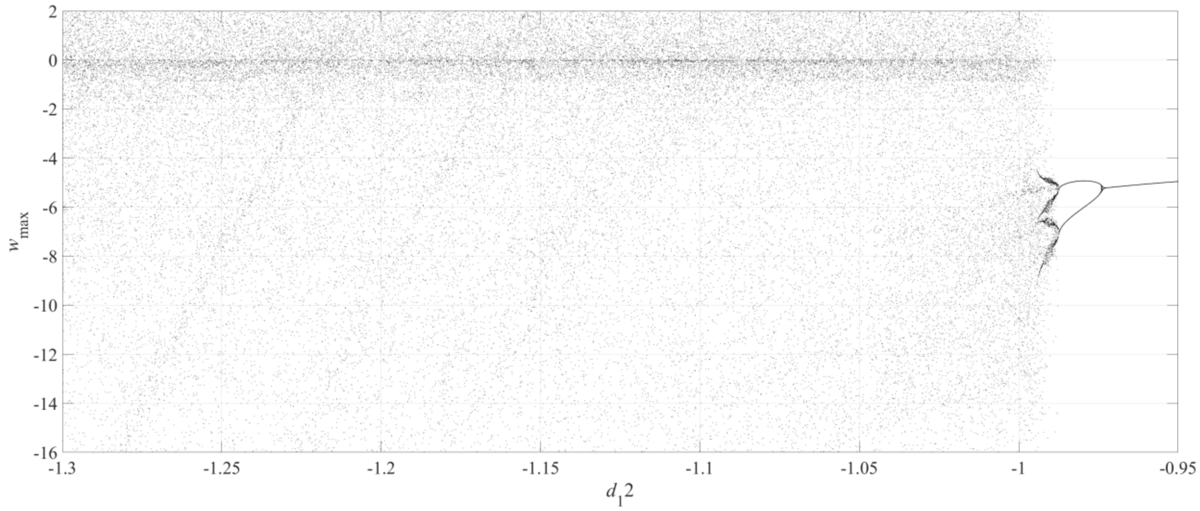

Fig. 19. Bifurcation diagram for hyperchaotic attractor hyper #2.

Finally, the hyperchaotic attractor hyper #3 is shown in Fig. 20. As in the case of hyper #2, this attractor also has a complex structure, but it is more compact in terms of phase space.

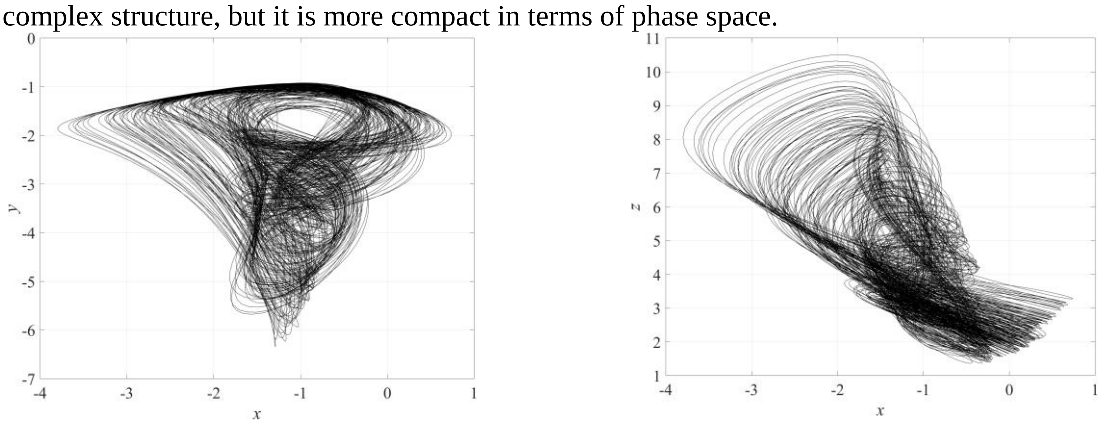

(a) XY plane

(b) XZ plane

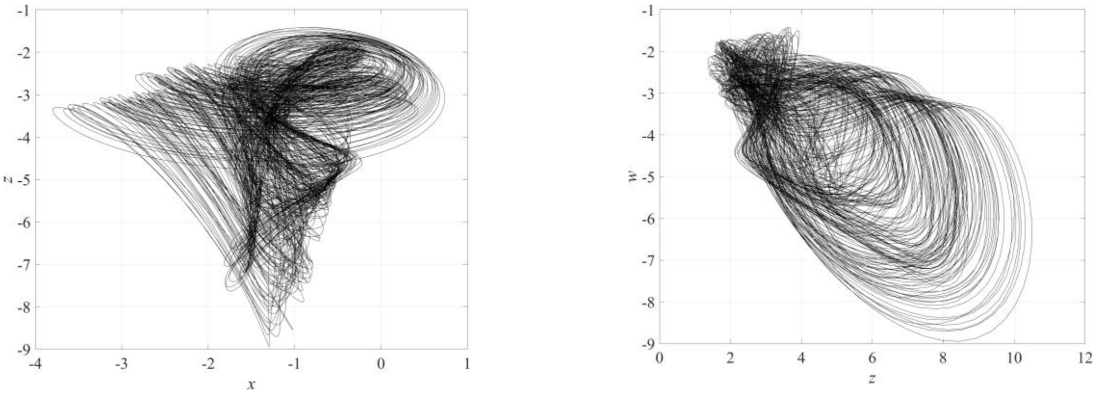

(c) XW plane (d) ZW plane

Fig. 20. Hyperchaotic attractor hyper #3.

The LEs are shown in Figure 21. The Kaplan-Yorke dimension is equal to 3.1488.

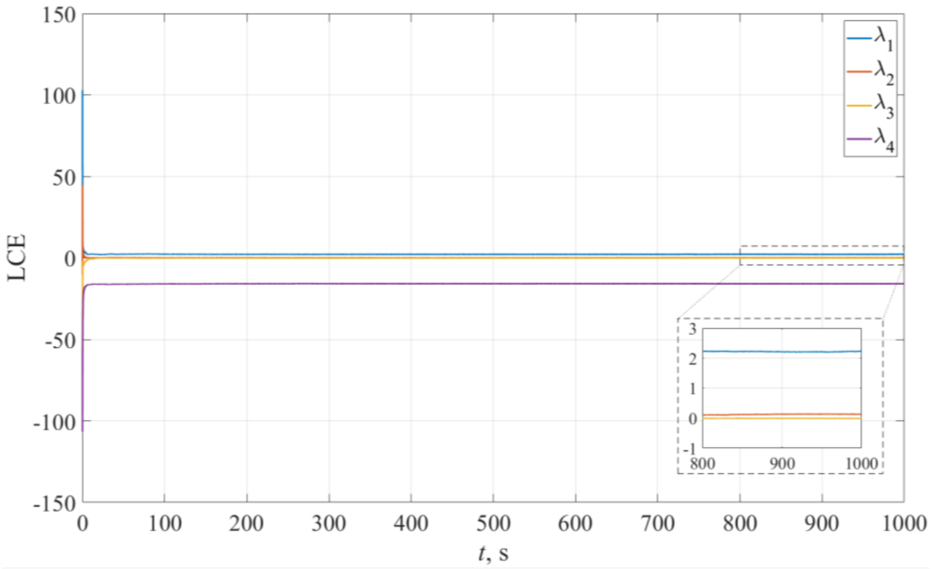

Fig. 21. LEs for hyperchaotic attractor hyper #3.

Bifurcation diagram for hyperchaotic attractor hyper #3 is shown in Fig. 22. As can be seen from Fig. 22, hyperchaotic attractor hyper #3 has two stable zones in the considered range.

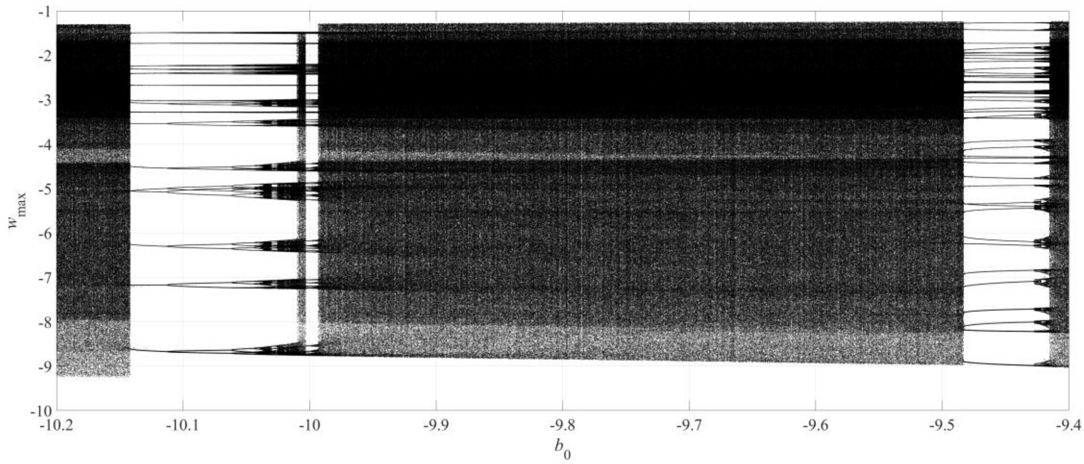

Fig. 22. Bifurcation diagram for hyperchaotic attractor hyper #3.

3.2. *Generation of a strange attractor using an indirect approach*

As in the previous "direct" approach, the system of differential equations was numerically solved using a fourth-order Runge–Kutta integration scheme. The integration step is also set constant and equal to 0.001 s. The numerical calculations were performed using the MATLAB program.

The population size N for the differential evolution algorithm is equal to the number of control coefficients multiplied by 20. The mutation and crossover parameters are similar to the direct approach and are set to $F = 0.5$ and $P = 0.99$, respectively.

The new strange chaotic attractors obtained in accordance with Eq. (13) are attractors with a minimum phase volume (we call such attractors a “MPV” – “minimal phase volume”). Strange attractors obtained in accordance with Eq. (35) are attractors with a minimum of control parameters from vector **U** (we call such attractors a “MCV” – “minimal control values”).

So, let us synthesize the first two new attractors MPV #1 and MCV #1 at the following hypothetical parameters of the spacecraft (22): $A = 50$, $B = 70$, $C = 90$. The obtained strange attractors have a two-scroll structure (Fig. 23).

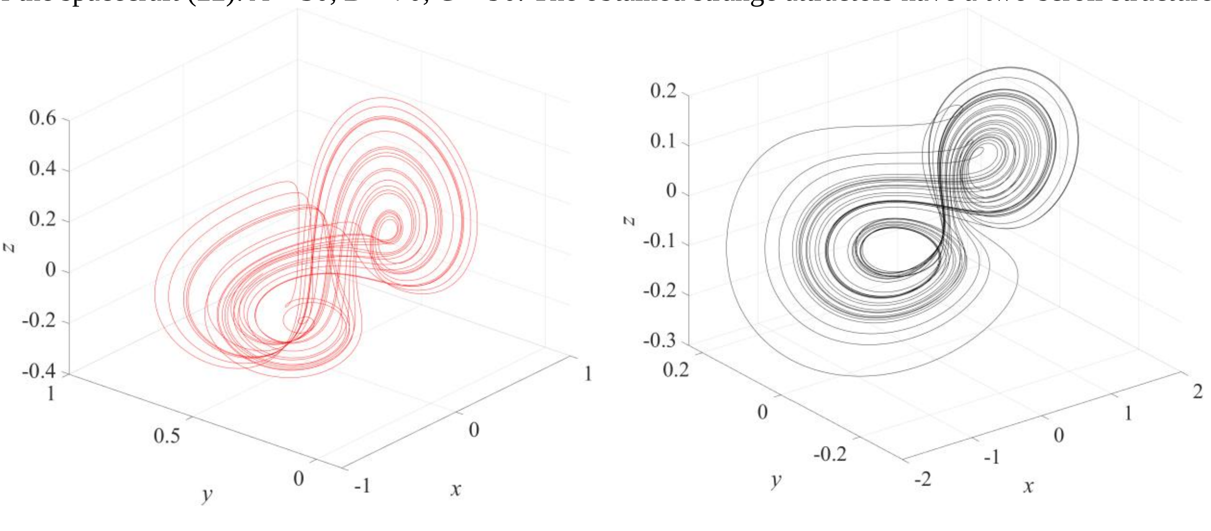

(a) MPV #1 (b) MCV #1

Fig. 23. Comparison of strange attractors.

LEs for MPV #1 and MCV #1 attractors are shown in Fig. 24. The Kaplan-Yorke dimension is equal to 2.215 and 2.137 for MPV #1 and MCV #1 attractors, respectively.

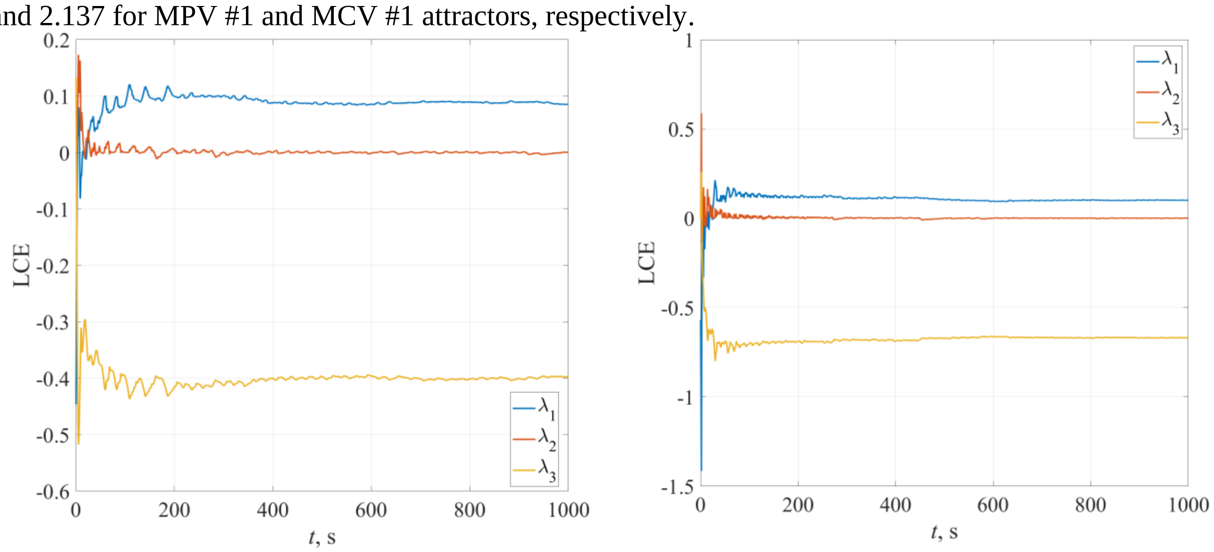

(a) MPV #1 (b) MCV #1

Fig. 24. LEs for the generated attractors.

Below are presented the bifurcation diagrams for MPV #1 and MCV #1 attractor (Fig. 25) at varying the coefficient a_0 at all fixed others coefficients, where we see notable differences in their structures and ranges of the chaotic behavior.

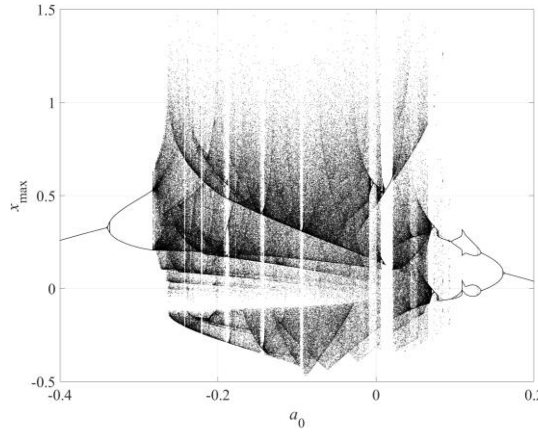

(a) 1D bifurcation diagram for MPV #1

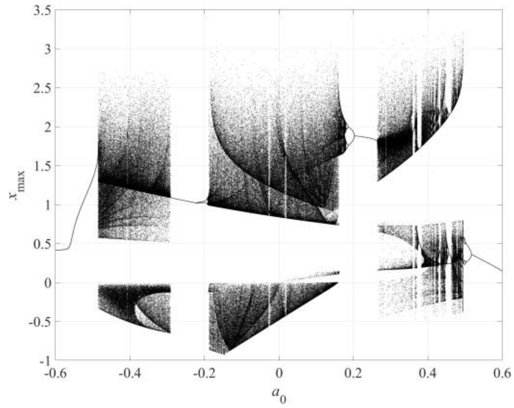

(b) 1D bifurcation diagram for MCV #1

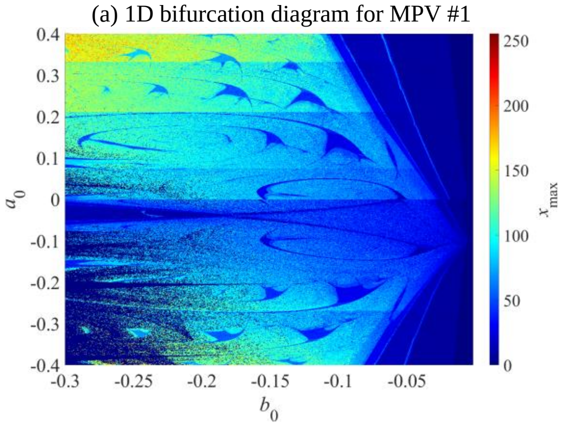

(c) 2D bifurcation diagram for MPV #1 (закрыть пробел)

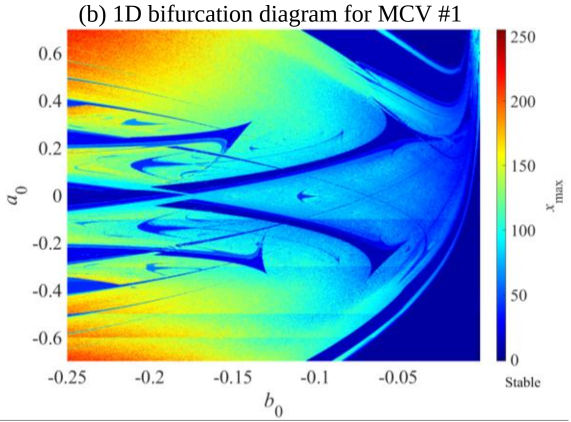

(d) 2D bifurcation diagram for MCV #1

Fig. 25. Bifurcation diagrams.

Let us find one more pair of strange attractors which can be used in the framework of attitude dynamics. In this regard, it is necessary to simplify the structure of possible control and, for these purposes, to minimize the number of nonlinear terms in Eq. (1). To reduce the number of nonlinear terms, we can set the coefficient c_7 to zero. To zero out the coefficient c_7, we assume that $\alpha_p = 0$, and $\beta_q = B - A$. Then, using the differential evolution algorithm, we can obtain new MPV#2 and MCV#2. The phase space of MPV #2 and MCV #2 is depicted in Fig. 26, and the corresponding parameters are collected in Tables 6 and 7.

Despite the increased control coefficients, MPV #2 has significantly lower values of phase variables (Fig. 26).

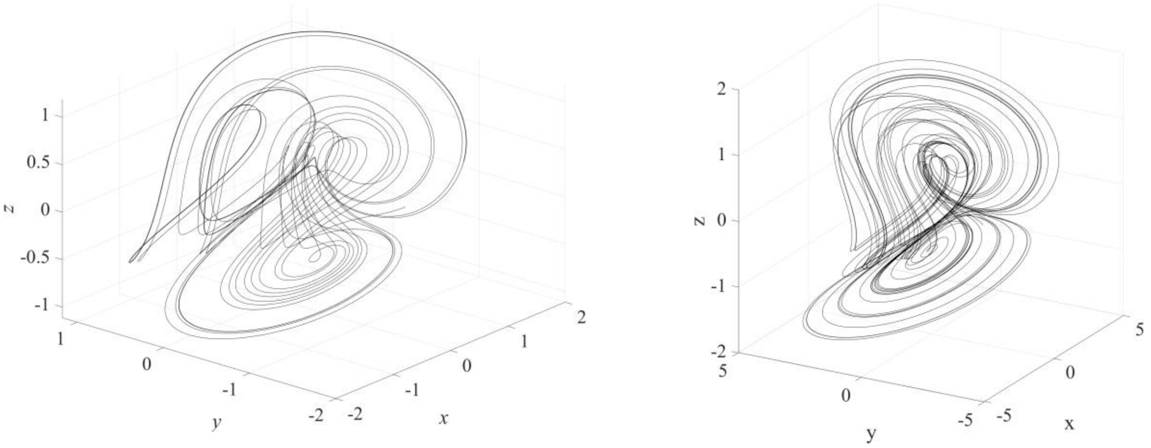

(a) MPV #2 (b) MCV #2

Fig. 26. Phase space.

LEs for MPV #2 and MCV #2 attractors are shown in Fig. 27. The Kaplan-Yorke dimension is equal to 2.3 and 2.242 for MPV #2 and MCV #2 attractors, respectively.

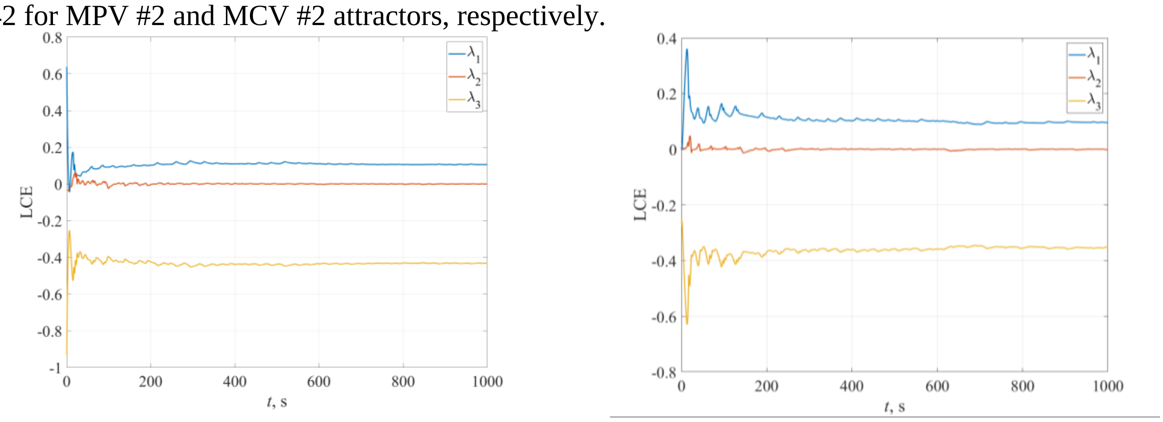

(a) (b)

Fig. 27. LEs **a** for the MPV #2 attractor and **b** for the MCV#2 attractor.

MPV #2 and MCV #2 have a typical bifurcation diagram (Fig. 28a and Fig. 28b, respectively).

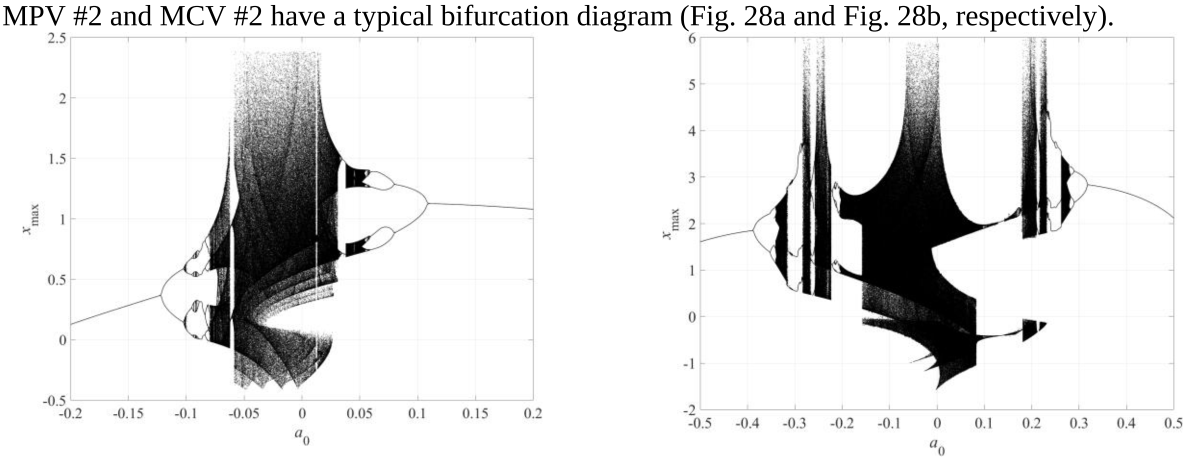

(a) 1D bifurcation diagram for MPV #2 (b) 1D bifurcation diagram for MCV #2

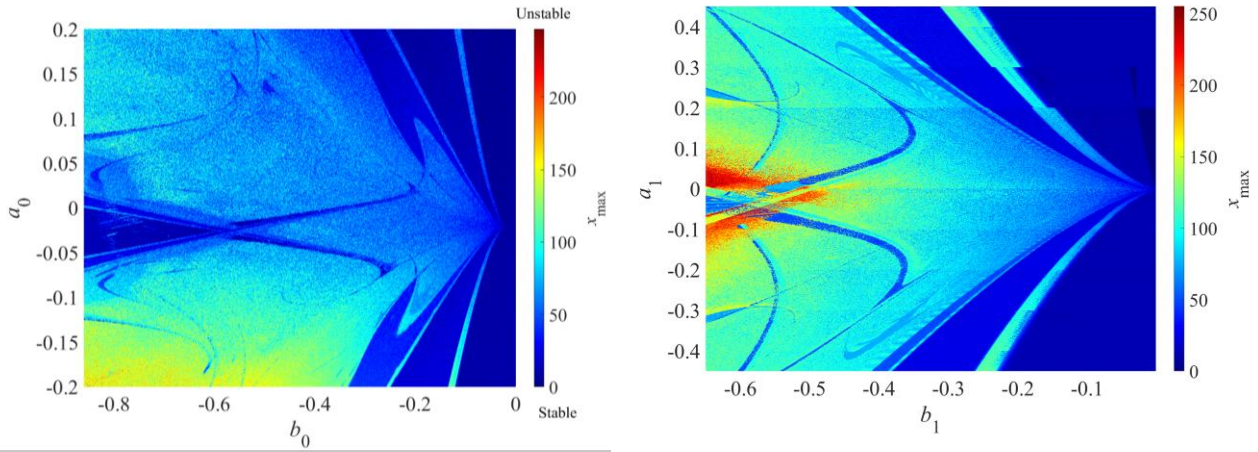

(c) 2D bifurcation diagram for MPV #2

(d) 2D bifurcation diagram for MCV #2

Fig. 28. Hyperchaotic strange attractor hyper #3.

4. Conclusion

In this paper, two approaches for synthesizing dynamical systems with strange chaotic attractors are presented. In both approaches, the generation of such attractors was performed using the differential evolution algorithm.

Notably, the direct approach searches system coefficients in a general sense, allowing them to be varied and assigned without regard to physical constraints. In other words, coefficients may be chosen arbitrarily, provided that the desired result is achieved.

The indirect approach, by contrast, precludes such arbitrariness. Here, the coefficients correspond to specific quantities within a given dynamical system and are subject to relationships and interdependencies. They possess clear physical meanings and are governed by established physical laws. Consequently, changes to these coefficients must be made comprehensively, respecting these interrelations. Coefficients are not varied arbitrarily; rather, specific coefficients are selected based on the physical context of the problem and align with the control laws of the dynamical system. For instance, the indirect approach is well suited to generating strange attractors in applied technical problems, such as the angular motion of a spacecraft under the influence of specific control forces. In such cases, meaningful opportunities for varying coefficients and their ranges emerge, although these variations are not arbitrary. A direct approach applied to dynamical systems arising from practical problems cannot be implemented without accounting for the interdependencies among system coefficients and the governing laws of the system's parameters.

This underscores the fundamental distinction between the two approaches: arbitrariness characterizes the direct approach, whereas interdependence defines the indirect approach.

Notably, the direct approach can be extended to higher-dimensional systems (4D and above), enabling the synthesis of hyperchaotic strange attractors. Such systems are of interest both for practical applications and for advancing fundamental approaches to studying chaotic dynamics.

The novelty of the approaches and results lies in the ability to generate any strange chaotic attractor with predetermined properties, such as the desired fractal dimension, minimal phase volume, or minimal control parameters. In other words, the results extend beyond specific cases and apply to all generated attractors. Thus, the presented approaches can generate not merely new attractors (i.e., systems with new sets of coefficients), but attractors with prescribed properties—a new capability that has not been demonstrated in previous works.

Acknowledgments

This work was supported by the Russian Science Foundation (# 25-19-00312).

Limitations and Future works

The limitations of this article primarily concern the types of mathematical models used to search for strange chaotic attractors: three-dimensional and four-dimensional systems of ordinary differential equations with quadratic nonlinearities—herein referred to as Sprott systems.

In the indirect approach, a system of equations for the angular motion of a spacecraft with flywheels was also used, employing specific control methods for the flywheels' relative angular momentum and a specific type of control force dependence. Notably, the developed approaches can be further applied to other types of control laws.

Future research directions include: (i) the exploration of broader classes of mathematical models governed by systems of ordinary differential equations with alternative nonlinearities—for instance, mixed polynomial nonlinearities of order exceeding two; (ii) the extension of the proposed approaches to a wider range of technical applications; (iii) the development of mathematical models that allow limiting hyperchaotic attractors using an indirect approach; and (iv) the development of more general control laws applicable to such systems. Of particular significance is the prospect of synthesizing dynamical systems with prescribed properties of strange chaotic attractors, a capability that underpins the broader utility of the presented methodologies.

Authors Contributions

Anton V. Doroshin: Conceptualization, Validation, Supervision, Writing – review & editing.
Nikolay A. Elisov: Conceptualization, Investigation, Software, Writing – original draft.

Competing Interests

The authors declare that they have no conflict of interest.

Data Availability

Data generated during this study will be made available on reasonable request.

ORCID

Anton V. Doroshin – https://orcid.org/0000-0001-6310-0963
Nikolay A. Elisov – https://orcid.org/0000-0002-4094-794X

Appendix A. Strange attractor coefficients and initial conditions

The initial conditions for the generated strange attractors are given in Table A1. The variable w is only applicable for attractors labeled a “hyper”.

Table A1. Initial conditions.

Attractor	x	y	z	w
Unoptimized attractor #1 Optimized attractor #1 Unoptimized attractor #2 Optimized attractor #2 Unoptimized attractor #3 Optimized attractor #3 MPV #1 MCV #1 MPV #2 MCV #2	0.05	0.1	0.09	—
Hyper #1 Hyper #2	0.05	0.1	0.09	0.3
Hyper #3	1	1	1	1

The comparison of coefficients for Eq. (1) between the unoptimized #1 and optimized #1 chaotic attractors is given in Table A2.

Table A2. Coefficients of the complete system.

Parameter	Unoptimized attractor #1	Optimized attractor #1
Coefficients a_i	a_0 = 6.81, a_1 = 0.36, a_2 = -8.77, a_3 = 2.02, a_4 = 7.02, a_5 = -8.83, a_6 = -0.26, a_7 = 2.7, a_8 = -5, a_9 = 0.02	a_0 = 0, a_1 = -3.7, a_2 = 7.5832, a_3 = 0.6705, a_4 = 2.9, a_5 = -6.7, a_6 = -3.8, a_7 = -6, a_8 = -7.1, a_9 = -0.5
Coefficients b_i	b_0 = -1.89, b_1 = 0.93, b_2 = 4.76, b_3 = 0.64, b_4 = 9.99, b_5 = -0.22, b_6 = -4.35, b_7 = -0.28, b_8 = 7.11, b_9 = -9.08	b_0 = 1.1, b_1 = -8.3707, b_2 = -6, b_3 = -2.5, b_4 = 7.4, b_5 = 7, b_6 = -0.6, b_7 = 6.6, b_8 = -9.3, b_9 = -8.5
Coefficients c_i	c_0 = -4.74, c_1 = -1.3, c_2 = -6.28, c_3 = -0.31, c_4 = 6.27, c_5 = 8.95, c_6 = -3.37, c_7 = -2.32, c_8 = 1.26, c_9 = 6.93	c_0 = 0.3, c_1 = -8.5, c_2 = 6.1, c_3 = -3.1298, c_4 = -6, c_5 = 9.9, c_6 = 4.1, c_7 = 0.1, c_8 = -0.6, c_9 = 6

Coefficients of the unoptimized #2 and optimized #2 strange attractors are presented in Table A3. The non-mentioned coefficients from Eq. (1) are zero.

Table A3. Coefficients of the reduced system.

Parameter	Unoptimized attractor #2	Optimized attractor #2
Coefficients a_i	a_1 = -0.7089, a_2 = 0.351, a_9 = 0.2291	a_1 = -0.4, a_2 = 1, a_9 = 20.8
Coefficients b_i	b_1 = -0.1769, b_2 = -0.7795, b_3 = -0.0205, b_8 = 0.4831	b_1 = 0.5, b_2 = -1.3, b_3 = 0.1, b_8 = 26.9
Coefficients c_i	c_2 = -0.0824, c_3 = 0.5607, c_7 = -0.4076	c_3 = 0.6, c_7 = -23.1

The coefficients for the unoptimized #3 and optimized #3 attractors are presented in Table A4.

Table A4. Coefficients of Thomas-like attractors.

Parameter	Unoptimized attractor #3	Optimized attractor #3
Coefficients a_i	$a_1 = -0.92$, $a_2 = a_3 = -5$	$a_1 = -5.1$, $a_2 = -1.4$, $a_3 = -49.2$
Coefficients b_i	$b_1 = -0.94$, $b_2 = b_3 = -5$	$b_1 = -4.1$, $b_2 = -0.6$, $b_3 = -30.7$
Coefficients c_i	$c_1 = -1.03$, $c_2 = c_3 = -5$	$c_1 = -8.9$, $c_2 = -1.7$, $c_3 = -45.2$

The coefficients of MPV #1 and MCV #1 are collected in Table A5, and the corresponded control components **U** are presented in Table A6.

Table A5. Coefficients of MPV #1 and MCV #1 chaotic attractors.

Parameter	MPV #1	MCV #1
Coefficients a_i	$a_0 = -0.0209$, $a_1 = -0.4461$ $a_2 = -0.0701$, $a_3 = 1.0626$, $a_9 = 0.6065$	$a_0 = 0.0154$, $a_1 = -0.5689$ $a_2 = 0.3348$, $a_3 = 5.8206$, $a_9 = -36.9297$
Coefficients b_i	$b_0 = -0.0583$, $b_1 = -0.0225$, $b_2 = 0.0013$, $b_3 = 0.1318$, $b_8 = 1.5168$	$b_0 = -0.06$, $b_1 = -0.0026$ $b_2 = 7.0905 \cdot 10^{-4}$, $b_3 = -0.0027$, $b_8 = 1.2787$
Coefficients c_i	$c_0 = 0.0187$, $c_1 = 0.286$, $c_2 = -0.1103$, $c_3 = 0.1332$, $c_7 = -1.1059$	$c_0 = 0.0022$, $c_1 = -0.0351$, $c_2 = 0.0021$, $c_3 = 4.95 \cdot 10^{-4}$, $c_7 = -0.7713$

Table A6. Components of the control vector **U** for MPV #1 and MCV #1.

Parameter	MPV #1	MCV #1
First group	$\alpha_0 = -18.0694$, $\alpha_1 = 19.6707$, $\alpha_p = -94.0932$, $m_x = 1.2774$	$\alpha_0 = 0.1899$, $\alpha_1 = -0.3092$, $\alpha_p = -49.4565$, $m_x = 0.0084$
Second group	$\beta_0 = -46.8516$, $\beta_1 = 0.1845$, $\beta_q = 67.0763$, $m_y = -7.9892$	$\beta_0 = 3.1637$, $\beta_1 = 0.0497$, $\beta_q = 0.0746$, $m_y = -4.2073$
Third group	$\gamma_0 = -3.0889$, $\gamma_1 = 21.8245$, $\gamma_r = 73.8181$, $m_z = 3.0681$	$\gamma_0 = -0.182$, $\gamma_1 = 0.0446$, $\gamma_r = 0.1472$, $m_z = 0.1981$

The coefficients of MPV #2 and MCV #2 are presented in Table A7. The control components **U** for initialization of these strange attractors are presented in Table A8.

Table A7. Coefficients of MPV #2 and MCV #2 chaotic attractors.

Parameter	MPV #2	MCV #2
Coefficients a_i	$a_0 = -0.0017$, $a_1 = 0.6388$, $a_2 = 0.0226$, $a_3 = -1.3385$, $a_9 = -0.8$	$a_0 = -0.0163$, $a_1 = 0.0068$, $a_2 = -0.0055$, $a_3 = -0.3659$, $a_9 = -0.8$
Coefficients b_i	$b_0 = -0.1688$, $b_1 = -0.0226$, $b_2 = -0.0319$, $b_3 = -0.0401$, $b_8 = 0.8$	$b_0 = -0.3460$, $b_1 = 0.0055$, $b_2 = 5.6016 \cdot 10^{-4}$, $b_3 = 0.0125$, $b_8 = 0.8$
Coefficients c_i	$c_0 = -0.0275$, $c_1 = 0.7436$, $c_2 = 0.0223$, $c_3 = -0.9318$	$c_0 = -0.0042$, $c_1 = 0.2033$ $c_2 = -0.0069$, $c_3 = -0.2647$

Table A8. Components of the control vector **U** for MPV #2 and MCV #2.

Parameter	MPV #2	MCV #2
First group	α_0 = 2.0053, α_1 = 31.9399, α_p = 0, m_x = -0.0859	α_0 = -0.6247, α_1 = 0.3395, α_p = 0, m_x = -0.8152
Second group	β_0 = -66.927, β_1 = -1.5942, β_q = -20, m_y = -8.4383	β_0 = -18.2933, β_1 = 0.0280, β_q = -20, m_y = -17.3023
Third group	γ_0 = -1.1283, γ_1 = -83.858, γ_r = 0, m_z = -2.4733	γ_0 = 0.2753, γ_1 = -23.8197, γ_r = 0, m_z = -0.3774

Finally, coefficients for hyperchaotic attractors hyper #1 and hyper #2 are given in Table A9, and coefficients for hyper #3 are presented in Table A10.

Table A9. Coefficients of hyperchaotic attractors.

Parameter	hyper #1	hyper #2
Coefficients a_i	a_1 = -1.4671, a_2 = 1.6964, a_4 = 1.6871, a_{12} = 18.8371	a_1 = -1.5594, a_2 = 0.1339, a_4 = 1.3937, a_{12} = 0.8051
Coefficients b_i	b_1 = -0.8102, b_2 = -0.2776, b_3 = 0.321, b_{10} = 27.6176	b_1 = -0.3887, b_2 = -1.6789, b_3 = 0.8825, b_{10} = 0.2262
Coefficients c_i	c_3 = 0.301, c_9 = -21.0711	c_2 = -0.7817, c_3 = 0.9612, c_9 = -0.3504
Coefficients d_i	d_0 = 0.0584, d_{14} = -7.6644	d_4 = -1.5248, d_{12} = -1.2651

Table A10. Coefficients of the hyperchaotic attractor.

Parameter	hyper #3
Coefficients a_i	a_0 = 11.0396, a_1 = 17.5755, a_2 = 18.4956, a_3 = 12.4474, a_4 = -0.7367, a_5 = 11.3726, a_6 = -7.0334, a_7 = -6.2584, a_8 = 11.0239, a_9 = 10.5485, a_{10} = 0, a_{11} = 2.3537, a_{12} = 7.6857, a_{13} = -7.2758, a_{14} = -6.7635
Coefficients b_i	b_0 = -10.2365, b_1 = -4.8292, b_2 = 19.5598, b_3 = 3.5632, b_4 = 9.9173, b_5 = -10.6243, b_6 = -12.7785, b_7 = -4.0310, b_8 = -10.5971, b_9 = 5.0088, b_{10} = 1.7316, b_{11} = 10.2682, b_{12} = -14.0479, b_{13} = 3.6073, b_{14} = -11.8381
Coefficients c_i	c_0 = -17.886, c_1 = 14.8339, c_2 = -7.6937, c_3 = -8.1545, c_4 = 16.0517, c_5 = -6.3249, c_6 = 17.6219, c_7 = -7.0683, c_8 = -12.4787, c_9 = 0.1590, c_{10} = -6.2070, c_{11} = -9.9047, c_{12} = -2.3457, c_{13} = 5.0259, c_{14} = -15.51
Coefficients d_i	d_0 = 11.2356, d_1 = 18.3764, d_2 = 4.7404, d_3 = -5.6049, d_4 = -15.4599, d_5 = -15.985, d_6 = -8.2796, d_7 = 9.4307, d_8 = -11.8735, d_9 = -3.8327, d_{10} = 5.4518, d_{11} = -18.0053, d_{12} = 10.1317, d_{13} = 12.296, d_{14} = -9.8029

Appendix B. Strange attractors with the desired Kaplan-Yorke dimension

Fig. B1 shows a strange attractor with the desired Kaplan-Yorke dimension of 2.05. The initial conditions are the same as for the above-mentioned strange attractors.

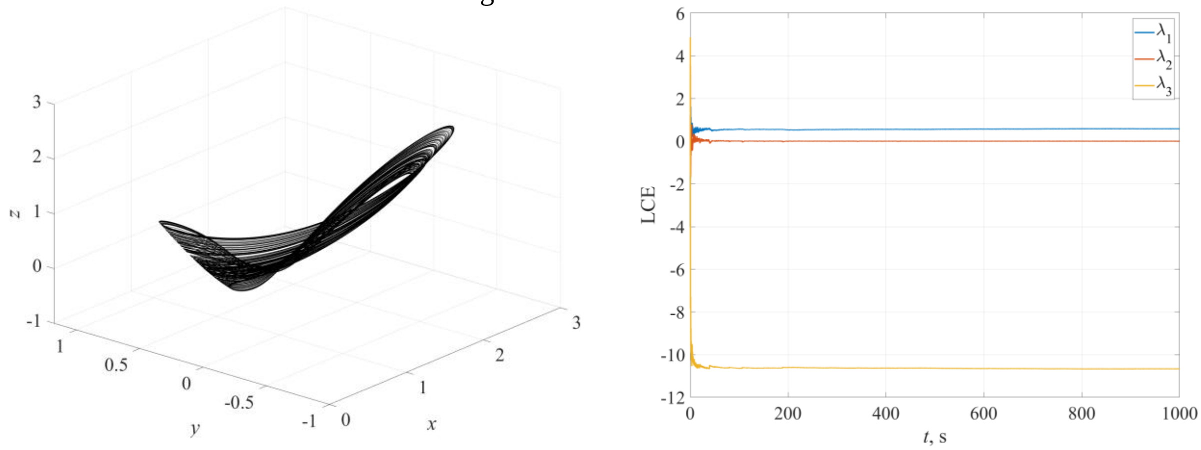

(a) Phase space (b) LEs

Fig. B1. Strange attractor with D_{KY} = 2.0541.

Fig. B2 shows a strange attractor with the desired Kaplan-Yorke dimension of 2.2.

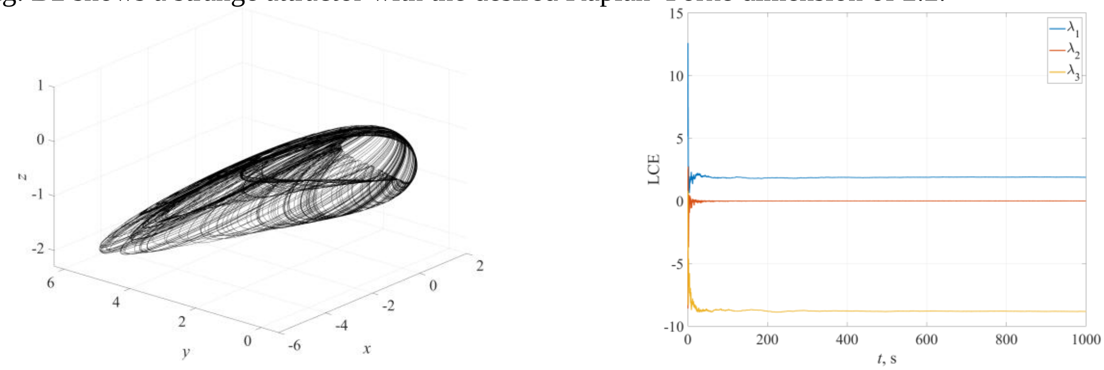

(a) Phase space (b) LEs

Fig. B2. Strange attractor with D_{KY} = 2.2142.

Fig. B3 shows a strange attractor with the desired Kaplan-Yorke dimension of 2.5.

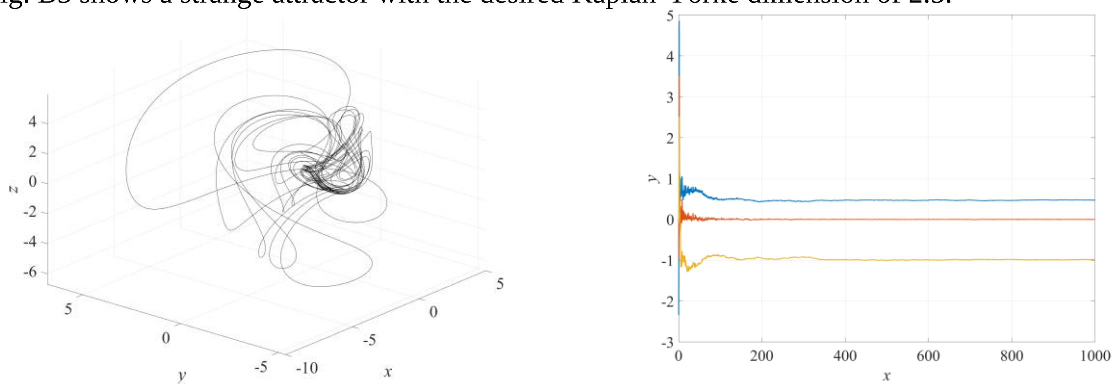

(a) Phase space (b) LEs

Fig. B3. Strange attractor with D_{KY} = 2.4838.

References

Aguilar-Ibanez, C., Suarez-Castanon, M.S., Saldivar, B., Valdez-Rodríguez, J.E., García-Canseco, E. [2025] "A DREM-based approach for the identification of chaotic systems" *Entropy* **27**, 971, https://doi.org/10.3390/e27090971.

Benettin, G., Galgani, L., Giorgilli, A., Strelcyn, J.M. [1980] "Lyapunov characteristics exponents for smooth dynamical systems and for hamiltonian systems; a method for computing all of them. Part 1: Theory," *Meccanica* **15**, pp. 9-20, https://doi.org/10.1007/BF02128236.

Benettin, G., Galgani, L., Giorgilli, A., Strelcyn, J.M. [1980] "Lyapunov characteristics exponents for smooth dynamical systems and for hamiltonian systems; a method for computing all of them. Part 2: Numerical application," *Meccanica* **15**, pp. 21-30, https://doi.org/10.1007/BF02128237.

Chua, L., Komuro, M., Matsumoto, T. [1986] "The double scroll family," *IEEE Trans. Circ. Syst*. **33**, pp. 1072-1118, https://doi.org/10.1109/TCS.1986.1085869.

Danca, M.F., Fěckan, M., Kuznetsov, N., Chen, G. [2021] "Attractor as a convex combination of a set of attractors," *Commun. Nonlinear Sci. Numer. Simul*. **96**, 105721, https://doi.org/10.1016/j.cnsns.2021.105721.

Doroshin, A.V. [2014] "Homoclinic solutions and motion chaotization in attitude dynamics of a multi-spin spacecraft," *Commun. Nonlinear Sci. Numer. Simul*. **19**, pp. 2528-2552, https://doi.org/10.1016/j.cnsns.2013.09.043.

Doroshin, A.V. [2015] "Initiations of chaotic regimes of attitude dynamics of multi-spin spacecraft and gyrostat-satellites basing on multiscroll strange chaotic attractors," *Proc. of IntelliSys – SAI Intelligent Systems Conference*, pp. 698-704, https://doi.org/10.1109/IntelliSys.2015.7361217.

Doroshin, A.V. [2016] "New strange chaotic attractors in dynamical systems of multi-spin spacecraft and gyrostats," *Proc. of IntelliSys – SAI Intelligent Systems Conference*, pp. 771-782, https://doi.org/10.1007/978-3-319-56994-9_53.

Doroshin, A.V. [2018] "Chaos as the hub of systems dynamics. The part I – The attitude control of spacecraft by involving in the heteroclinic chaos," *Commun. Nonlinear Sci. Numer. Simul*. **59**, pp. 47-66, https://doi.org/10.1016/j.cnsns.2017.11.008.

Doroshin, A.V. [2020] "Implementation of regimes with strange attractors in attitude dynamics of multi-rotor spacecraft," *Proc. of ITNT*, pp. 1-4, https://doi.org/10.1109/ITNT49337.2020.9253191.

Doroshin, A.V., Elisov, N.A. [2024] "Multi-rotor spacecraft attitude control by triggering chaotic modes on strange chaotic attractors," *Nonlinear Dyn*. **112**, pp. 4617-4649, https://doi.org/10.1007/s11071-024-09302-7.

Elhadj, Z., Sprott, J.C. [2013] "Simplest 3D continuous-time quadratic systems as candidates for generating multiscroll chaotic attractors," *Int. J. Bifurcat. Chaos*. **23**, pp. 1-6, https://doi.org/10.1142/S0218127413501204

Escudero, M., Spiga, S., Marco, M.D., Forti, M., Innocenti, G., Tesi, A., Corinto, F., Brivio, S. [2023] "Chua's circuit with tunable nonlinearity based on a nonvolatile memristor: design and realization," *IEEE TCAS-I* **71**, pp. 62-72, https://doi.org/10.1109/TCSI.2023.3323854.

Haken, H. [1975] "Analogy between higher instabilities in fluids and lasers," *Phys. Lett*. **53A**, pp. 77-78, https://doi.org/10.1016/0375-9601(75)90353-9.

Illing, L., Fordyce, R.F., Saunders, A.M., Ormond, R. [2012a] "Experiments with a Malkus-Lorenz water wheel: Chaos and Synchronization,", *Am. J. Phys*. **80**, pp. 192-202, https://doi.org/10.1119/1.3680533

Illing, L., Saunders, A.M., Hahs, D. [2012b] "Multi-parameter identification from scalar time series generated by a Malkus-Lorenz water wheel," *Chaos* **22**, 013127, http://dx.doi.org/10.1063/1.3689441

Kaplan, J.L., Yorke, J.A. [1979] "Chaotic behavior of multidimensional difference equations," Proc. of Functional Differential Equations and Approximation of Fixed Points, pp, 204-227, https://doi.org/10.1007/BFb0064319.

Karimov, A., Rybin, V., Kopets, E., Karimov, T., Nepomuceno, E., Butusov, D. [2023] "Identifying empirical equations of chaotic circuit from data" *Nonlinear Dyn*. **111**, pp. 871-886, https://doi.org/10.1007/s11071-022-07854-0

Kennedy, M.P. [1993] "Three steps to chaos – Part I: Evolution," *IEEE TCAS-I* **40**, pp. 640-656, https://doi.org/10.1109/81.246140.

Kennedy, M.P. [1994] "Chaos in the Colpitts oscillator," *IEEE TCAS-I* **41**, pp. 771-774, https://doi.org/10.1109/81.331536

Keuninckx, L, Van der Sande, G., Danckaert, J. [2014] "A simple two-transistor chaos generator based on a resistor-capacitor phase shift oscillator," *Proc. of NOLTA 2014*, pp. 490-493, https://doi.org/10.34385/proc.46.C2L-A4.

Keuninckx, L, Van der Sande, G., Danckaert, J. [2015] "Simple two-transistor single-supply resistor-capacitor chaotic oscillator," *IEEE TCAS-II* **62**, pp. 891-895, https://doi.org/10.1109/TCSII.2015.2435211.

Kramer, S., Bollt E.M. [2013] "Spatially dependent parameter estimation and nonlinear data assimilation by autosynchronization of a system of partial differential equations," *Chaos* **23**, 033101, https://doi.org/10.1063/1.4812722

Kuznetsov, N., Mokaev, T., Ponomarenko, V., Seleznev, E., Stankevich, N., Chua, L. [2023] "Hidden attractors in Chua circuit: mathematical theory meets physical experiments," *Nonlinear Dyn*. **111**, pp. 5859-5887, https://doi.org/10.1007/s11071-022-08078-y.

Li, C., Sprott, J.C. [2013] "Chaotic flows with a single nonquadratic term," *Phys. Lett. A* **378**, pp. 178-183, https://doi.org/10.1016/j.physleta.2013.11.004.

Li, C., Sprott, J.C. [2017] "An infinite 3-D quasiperiodic lattice of chaotic attractors," *Phys. Lett. A* **382**, pp. 581-587, https://doi.org/10.1016/j.physleta.2017.12.022.

Lorenz, E.N. [1963] "Deterministic nonperiodic flow," *J. Atmos. Sci.* **20**, pp. 130-141, https://doi.org/10.1175/1520-0469(1963)020<0130:DNF>2.0.CO;2.

Ma, X., Li, C., Li, Y., Bi, L., Qi, Z. [2022] "Rotation control of an HR neuron with a locally active memristor," *Eur. Phys. J. Plus* **137**, 542, https://doi.org/10.1140/epjp/s13360-022-02761-0.

Marco, M.D., Forti, M., Pancioni, L., Innocenti, G., Tesi, A., Corinto, F. [2022] "Oscillatory circuits with a real non-volatile Stanford memristor model," *IEEE Access*. **10**, pp. 13650-13662, https://doi.org/10.1109/ACCESS.2022.3146419.

Matsumoto, T. A [1984] "Chaotic attractor from Chua's circuit," *IEEE Trans. Circuits Syst*. **31**, pp. 1055-1058, https://doi.org/10.1109/TCS.1984.1085459.

Matsumoto, T., Chua, L., Komuro, M. [1985] "The double scroll," *IEEE Trans. Circ. Syst*. **32**, pp. 797-818, https://doi.org/10.1109/TCS.1985.1085791.

Maxwell, J.C. [1995] *Does the progress of physical science tend to give any advantage to the opinion of necessity (or determinism) over that of the contingency of events and the freedom of the will?* (Cambridge University Press, UK).

Medvinsky, A.B., Petrovskii, S.V., Tikhonova I.A., Malchow, H., Li, B.-L. [2002] "Spatiotemporal complexity of plankton and fish dynamics," *SIAM Review* **44**, pp. 311-370, https://doi.org/10.1137/S0036144502404442

Mobayen, S., Volos, C.K., Kaçar, S., Çavuşoğlu, Ü. [2018] "New class of chaotic systems with equilibrium points like a three-leaved clover," *Nonlinear Dyn*. **91**, pp. 939-956, https://doi.org/10.1007/s11071-017-3920-4.

Niyat, A.Y., Moattar, M.H. [2020] "Color image encryption based on hybrid chaotic system and DNA sequences," *Multimed. Tools Appl*. **79**, pp. 1497-1518, https://doi.org/10.1007/s11042-019-08247-z.

Petrzela, J. [2016] "On the existence of chaos in the electronically adjustable structures of the state variable filters," Int. J. Circ. Theor. Appl. **44**, pp. 1779-1797, https://doi.org/10.1002/cta.2193

Pham, V.-T., Jafari, S., Volos, C., Kapitaniak, T. [2016] "A gallery of chaotic systems with an infinite number of equilibrium points," *Chaos Solit. Fractals* **93**, pp. 58-63, https://doi.org/10.1016/j.chaos.2016.10.002.

Poincaré, H. [2017] *Three-body problem and the equations of dynamics: Poincaré's foundational work on dynamical systems theory* (Springer, Germany).

Qu, Z., Li, C., Wang, L., Xue, Y., Qi, X. [2025] "Constructing nonuniform multiscroll chaotic strings," *Int. J. Bifurcat. Chaos* **35**, 2630005, https://doi.org/10.1142/S0218127426300053.

Rocha, R., Medrano-T, R.O. [2022] "Chua circuit based on the exponential characteristics of semiconductor devices," *Chaos Solit. Fractals* **156**, 111761, https://doi.org/10.1016/j.chaos.2021.111761.

Rössler, O.E. [1976] "An equation for continuous chaos," *Phys. Lett. A.* **57**, pp. 397-398, https://doi.org/10.1016/0375-9601(76)90101-8.

Sprott, J.C. [1993] "Automatic generation of strange attractors," *Comput. Graph.* **17**, pp. 325-332, https://doi.org/10.1016/0097-8493(93)90082-K.

Sprott, J.C. [1994] "Some simple chaotic flows," *Phys. Rev. E.* **50**, pp. 647-650, https://doi.org/10.1103/PhysRevE.50.R647.

Sprott, J.C. [1997] "Simplest dissipative chaotic flow," *Phys. Lett. A.* **228**, pp. 271-274, https://doi.org/10.1016/S0375-9601(97)00088-1.

Sprott, J.C. [2000] *Strange attractors: creating patterns in chaos* (M&T Books, USA).

Storn, R., Price, K. [1997] "Differential evolution – a simple and efficient heuristic for global optimization over continuous spaces," *J. Glob. Optim.* **11**, pp. 341-359, https://doi.org/10.1023/A:1008202821328.

Thomas, R. [1999] "Deterministic chaos seen in terms of feedback circuits: Analysis, synthesis, "labyrinth chaos"," *Int. J. Bifurcat. Chaos.* **9**, pp. 1889-1905, https://doi.org/10.1142/S0218127499001383.

Wang, X., Chen, G. [2013] "Constructing a chaotic system with any number of equilibria," *Nonlinear Dyn.* **71**, pp. 429-436, https://doi.org/10.1007/s11071-012-0669-7.

Wang, N., Xu, D., Li, Z., Xu, Q. [2023] "A general configuration for nonlinear circuit employing current-controlled nonlinearity: Application in Chua's circuit," *Chaos Solit. Fractals* **177**, 114233, https://doi.org/10.1016/j.chaos.2023.114233.

Wang, N., Xu, D., Kuznetsov, N. V., Bao, H., Chen, M., & Xu, Q. [2023] "Experimental observation of hidden Chua's attractor" *Chaos Solit. Fractals,* **170**, 113427, https://doi.org/10.1016/j.chaos.2023.113427

Wu, X., Kan, H., Kurths, J. [2015] "A new color image encryption scheme based on DNA sequences and multiple improved 1D chaotic maps," *Appl. Soft. Comput.* **37**, pp. 24-39, https://doi.org/10.1016/j.asoc.2015.08.008.

Wu, J., Liao, X., Yang, B. [2018] "Image encryption using 2D Henon-Sine map and DNA approach," *Signal Process.* **153**, pp. 11-23, https://doi.org/10.1016/j.sigpro.2018.06.008.

Yang, Q., Qiao, X. [2019] "Constructing a new 3D chaotic system with any number of equilibria," *Int. J. Bifurc. Chaos* **29**, 1950060, https://doi.org/10.1142/S0218127419500603.

Zhang, S., Li, C., Zheng, J., Wang, X., Zeng, Z., Chen, G. [2021] "Generating any number of diversified hidden attractors via memristor coupling," *IEEE TCAS-I* **68**, pp. 4945-4956, https://doi.org/10.1109/TCSI.2021.3115662.

Zhang, Y., Hua, Z., Bao, H., Huang, H. [2024] "Multi-valued model for generating complex chaos and fractals," *IEEE TCAS-I* **71**, pp. 2783-2796, https://doi.org/10.1109/TCSI.2024.3378448

Zhong, G.-Q., Ayrom, F. [1985] "Experimental confirmation of chaos from Chua's circuit," *Int. J. Circuit Theory Appl.* **13**, pp. 93-98, https://doi.org/10.1002/cta.4490130109

Zhong, G.-Q. [1994] "Implementation of Chua's circuit with a cubic nonlinearity," *IEEE TCAS-I* **41**, pp. 934-941, https://doi.org/10.1109/81.340866.

Zhong, G.-Q., Wu, C.W., Chua, L.O. [1998] "Torus-doubling bifurcations in four mutually coupled Chua's circuits," *IEEE TCAS-I* **45**, pp. 186-193, https://doi.org/10.1109/81.661689.